BES ANALYSIS MEMO

Ψ(2S) Hadronic Decays Involving ω and ϕ and Strong DOZI Violation

Liu Feng

lfeng@hpws3.ihep.ac.cn

Div. 1, IHEP, CAS

Abstract

We presented the first measurements of the branching ratios of Ψ(2S) decays into $\omega\pi^+\pi^-$, $\phi\pi^+\pi^-$, ωK^+K^-, ϕK^+K^-, $\omega p\bar{p}$, $\phi p\bar{p}$ and ϕf_0, $\pi^0\pi^+\pi^-p\bar{p}$, $\eta\pi^+\pi^-p\bar{p}$ and $\eta p\bar{p}$, and observed the strong OZI and DOZI violation w.r.t. the naive $\omega \sim \phi$ mixing model in $\Psi(2S)$ decays, the violation factors $R = \frac{Br(\phi X)}{Br(\omega X)}$ to the model predictions are of about two order of magnitude higher for Ψ(2S) decays into $\omega\pi^+\pi^-$, $\phi\pi^+\pi^-$, ωK^+K^-, ϕK^+K^-, and for $\omega p\bar{p}$, $\phi p\bar{p}$, the violation is not serious, but the results coincide with the pQCD and large N_C QCD predictions. The ratios of $\Psi(2S)$ hadronic decay branching fractions to those of J/ψ into $\omega\pi^+\pi^-$, ϕK^+K^-, $\omega p\bar{p}$ and $\eta p\bar{p}$ are smaller than the perturbative QCD predictions by a factor of 2, while for ωK^+K^-, $\phi\pi^+\pi^-$, ϕf_0, $\phi p\bar{p}$, $\eta\pi^+\pi^-p\bar{p}$ and $\pi^0\pi^+\pi^-p\bar{p}$, the ratios are consistent with the perturbative QCD predictions within errors.

1 Introduction

1.1 Background

In Standard Model[1], leptons and quarks participate in weak interaction via charged $V-A$ currents. For leptons, the weak charged current

$$J^\mu = \bar{\psi}_\nu \gamma^\mu \frac{1}{2}(1-\gamma_5)\psi_l$$

is pure $V-A$ current, while for quarks, because the mixing of quarks, i.e, the quarks involving in interactions are not their mass eigenstate, the weak charged current

$$J_\mu = \bar{\psi}_u \gamma_\mu \frac{1}{2}(G_V - G_A\gamma_5)\psi_d$$

is not pure $V-A$ current, where G_V, G_A, are the weak coupling constants for the vector and axial-vector currents, respectively, for leptons $G_V = 1.0, G_A = 1.0$. Where ψ's stand for field operators, γ^μ, γ_5 are γ matrix.

Early in the 1960's, it was observed that in some hadron semileptonic decays with the strangeness changed and unchanged, $G_V \sim 0.98$, indeed it differs significantly from strickly theoritical prediction **one**: $1 - G_V \sim 0.02$. In order to account for the stangeness changining $\Delta S = 0$ and $\Delta S = 1$ weak decays, in 1963, Cabbibo first introduced the doublets (u, d')[2],

$$d' = \quad dcos\theta_c + ssin\theta_c,$$

$$s' = -dcos\theta_c + ssin\theta_c.$$

where the introduced parameter θ_c, the quark mixing angle, known as Cabbibo angle, can be determined from experiments, $sin\theta_c \sim 0.23$.

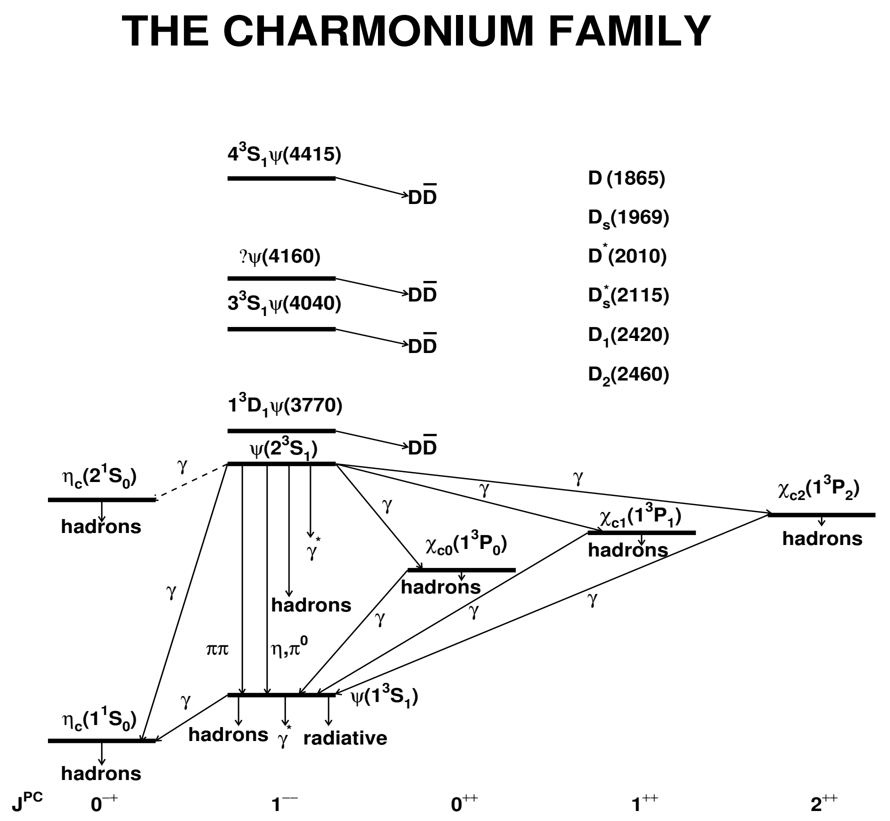

Figure 1: The Charmonium Family

In 1964, based on the aesthetic consideration of establishing a lepton-hadron parallelism (then (ν_e, e^-) and (ν_μ, μ^-) had been discovered), Bjorken and Glashow introduced charm quark[3]. But if there are only three quarks (u,d,s) , strangeness-changing neutral currents would inevitably arise in the effective current-current interaction Lagrangian, even Cabbibo mixing is taken into account. In 1970, in order to eliminate the unwanted strangeness-changing neutral currents, Glashow, Iliopoulos & Maiani(GIM)[4] introduced a new charmed quark c some years before its discovery, known as GIM mechanism. Cabbibo-GIM mechanism plays a very important role in flavor changing neutral currents (FCNC) even at higher orders, it ensures that there are no $s \leftrightarrow d$ transitions, which only change flavor but not charge. FCNC processes provide powerful tests of the Standard Model and physics beyound it.

In 1974, the so-called "November Revolution of Particle Physics", the 1^{--} groud state of the charmonium family, the J/ψ partilce, was discovered at Brookhaven, SLAC[5] and confirmed immediately afterwards at the ADONE and DORIS[6]. Soon after the discovery of the J/ψ, first the $\Psi(2S)$ and then a family of $c\bar{c}$-states[7], cf Fig. 1, were discoverd.

1.2 The OZI rule and $\omega \sim \phi$ mixing

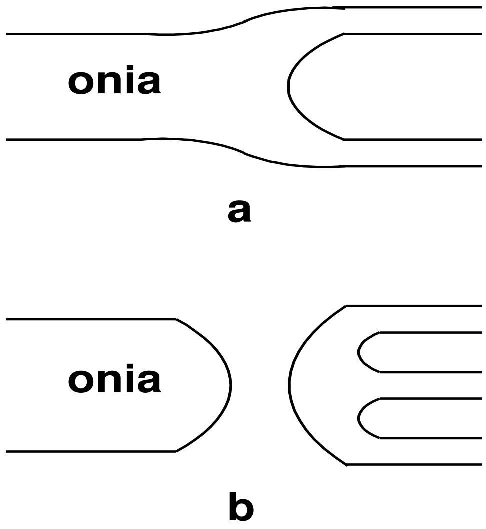

Figure 2: The OZI rule diagrams

The most surprising feature of these charmonia is their small decay widths which indicate the decays of charmonia into lighter hadrons are highly suppressed. The reason for the extremely small decay widths of charmonia is usually referred to by the phenomenological Okubo, Zweig and Iizuka (OZI) rule[8], it states that the processes with disconnected quark line in the initial or the final states are suppressed as compared to connected quark lines, the flavor disconnected processes means those are with extra quark loop. Diagrammatically this leads to a pictorial representation of the OZI rule, cf Fig. 2, the dominance of Fig. 2a over Fig. 2b. It phenomenologically explains the decay rate difference between $\phi \to 3\pi$ and $\phi \to K^+K^-$, and the narrow charmonium decay widths etc.

Apart from explaining the narrow decay widths of charmonia, the OZI rule plays an important role in the evaluation of hadronic charmonium decays, although all of the hadronic decays of the charmonia are singly OZI (SOZI) suppressed, some decays yet suffer another OZI suppression in the formation of the final state quarks, that is, the processes are doubly

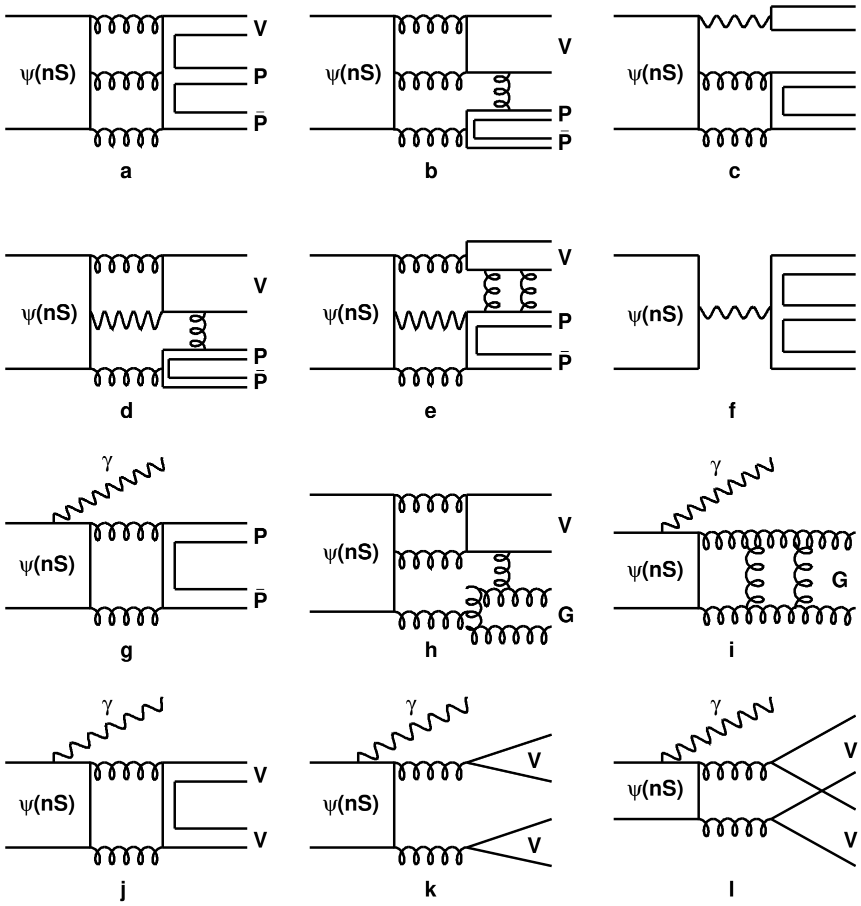

Figure 3: The lowest order digrams of charmonium decays. Charmonium decays into hadrons via (a) ggg, (b) ggg but DOZI suppressed, (c-e) electromagnetic decays into hadrons with (c) SOZI and (d,e) DOZI suppressed, (f) pure electromagnetic decays into hadrons, (g) radiative decays into hadrons, (h) hadronic decays into glueballs, (i) radiative decays into glueballs, (j-l) radiative decays into vector meson pairs. **NOTE:** two gluons can form glueballs, hybrids or $qq\bar{q}\bar{q}$ exotic states if no or one or two gluons split into quark-antiquark pairs. Where V stands for vector mesons, P for pseudoscalar mesons, G for glueballs.

OZI suppressed(DOZI). For example, the decay $\psi(nS) \to \phi\pi\pi$ is DOZI suppressed. In group theory, DOZI contribution corresponds to nonet symmetry breaking. A small DOZI amplitude can cause a large effect because of the interference with the large SOZI amplitude. Evidence in the decays of J/ψ into $\gamma + vector + vector$, such as $\gamma + \omega\phi$, shows DOZI is of much importance. The DOZI amplitude is about $0.3 \sim 0.5$ in $\gamma + vector + vector$ decay modes, and about ~ -0.15 for pseudoscalar$-$vector decay modes[9].

The strong interaction between quarks and gluons, was described by the non-Abelian gauge theory: Quantum Chromodynamics(QCD). Since gluons carry color charges (unlike photon which does not carry electric charge, so no interaction exists between photons), so gluons themselves can directly interact with other gluons which leads to an outstanding property of the asymptotic freedom, the basic feature of QCD, it means that perturbative calculations can be legitimately employed at short distance; Another feature is color confinement, that is, all hadron states are color-singlet. It is a consequence of the asymptotic freedom of QCD, since the strong interaction increases when the distance becomes larger.

Within the framework of Quantum Chromodynamics(QCD), for heavy quarks (c,b,t), the OZI suppression is due to the asymptotic freedom of QCD (see Fig. 3a) , because of their heavy mass, the momentum transfer q for heavy charm quark-antiquark pairs annihilation into light quarks via three gluons is higher, so the strong coupling constant $\alpha_s(q^2)$ is small, perturbative theory is applicable[11]. While the case of the strange quark belongs to the non-perturbative domain and involves more complicated dynamics. Since the charm mass is large, $m_c \sim 1.5$ GeV, the strong coupling constant $\alpha_s(m_c^2) \sim 0.3$, is not too small, charmonium physics is in the boundary domain between perturbative and non-perturbative QCD, it offers a good area to study non-perturbative QCD. There are several reasons that non-perturbative QCD is one of the interesting and hot subjects in current physics. From the birth of Quantum Chromodynamics (QCD), much progress has been made to reveal rich structure of QCD from asymptotic freedom to non-perturbative regions. However essential questions associated especially with non-perturbative properties such as quark confiments and chiral symmetry breaking are not fully understood. So since the discovery of charm, it attracts both theoritical and experimental attention, fruitful achievement has been obtained.

Charmonium decays allow a unique study of the hadron dynamics and the low mass meson spectroscopy and its pure hadronic decays have been usefull because of the clean surroundings where the initial state is well defined $J^{+-} = 1^{--}$. Moreover, $\Psi(2S)$ provides a powerful tool to study P-wave charmonia $\chi_{cJ}(J = 0, 1, 2)$.

The charmonia decays into vector-pseudoscalar-pseudoscalar finla states are expected to proceed mainly by two mechanisms: strong decays via $c\bar{c}$ annihilation into three gluons Fig. 3a, then they decay into hadrons; and the substantial contributions from the electromagnetic annihilation through one virtual photon Fig. 3f which then decays into hadrons. The electromagnetic contributions to the decays are important since the strong decays are OZI suppressed. Doubly OZI suppressed amplitudes (e.g. Fig. 3b,d,e) may also contribute to the decays rates for the interference between the DOZI and the large SOZI processess.

Because of the confinement and the non-Abelian characteristics of QCD, maybe the most dramatic and novel predictions of QCD are the existence of the colorless gg bound states (glueballs) and $q\bar{q}g$ bound states (hybrids) and multiquark $qq\bar{q}\bar{q}$ bound states along with the ordinary mesons and baryons. Another important decay is radiative decay modes of charmonia, cf Fig. 3i. The radiative decays of charmonia provide a suitable system to search for such unusual states and probe these QCD predictions, but the search for these composites is a longstanding problem. The radiative decay modes also offer a rich laboratory to study

$\eta_c(1S)$ or χ_{cJ} and search for $\eta_c(2S)$ and hadronic decays to look for $^1P_1$ states.

Out of the charmonium decays, there exists a mysterious and longstanding puzzle, known as $\rho\pi$ or vector-pseudoscalar puzzle, first revealed by Mark II[10]. The charnonia are the bound states of a charm quark and its antiquark. According to the perturbative QCD, the lowest-order diagrams for J/ψ and $\Psi(2S)$ decay into lighy hadrons proceed via c and $\bar{c}$ annihilation into ggg or a virtual photon. In such case, the partial decay width is proportional to the wave functions $\Psi(0)$ at the origin in the nonrelativistic quark model. based on the similarity between the $\Psi(2S)$ and J/ψ wave fuctions and the slow running of the strong coupling constant $\alpha_s(q^2)$, the ratios of the decay width of $\Psi(2S)$ decays into hadrons to that of J/ψ decays into hadrons can be expressed as[11]:

$$Q_h = \frac{Br(\Psi' \to h)}{Br(J/\psi \to h)} = \frac{Br(\Psi' \to e^+e^-)}{Br(J/\psi \to e^+e^-)} = (14.7 \pm 2.3)\%$$

which was named "15%" rule, where the leptonic branching fractions are taken from the PDG tables[12]. The observed results[10] of $\rho\pi$ and $K^\star\bar{K}$ with $Q_{\rho\pi} < 0.6\%$ and $Q_{K^\star\bar{K}} < 2\%$ significantly violate the theoritical predictions, BES confirms the results of $Q_{\rho\pi} < 0.23\%$, $Q_{K^\star\bar{K}} < 0.64\%$ and $Q_{K^\star\bar{K}^0} = (1.7{\pm}0.6)\%$ at higher precision and reveals new strong violation of "15%" rule in vector plus tensor decay modes[13]. Various theoritical models[14] have been put forward to explain the puzzle, but none of them is satisfactory.

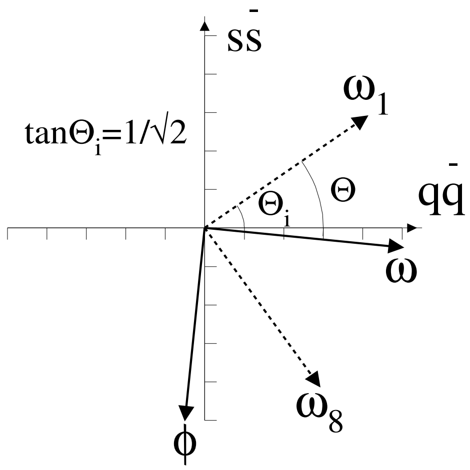

Figure 4: $\omega \sim \phi$ mixing

In recent years, the abundant ϕ meson production in nucleon-antinucleon and meson-nucleon annihilation were experimentally observed[15]. Of special interest are the processes resulting in the violation of the Okubo-Zweg-Iizuka (OZI) rule, while some channels, e.g, ($\phi\pi$, $\phi\gamma$, $\phi\rho$, $\omega\phi$, $\phi\phi$), are expected to be DOZI or OZI-suppressed in the tree level, because ϕ is dominantly a pure $s\bar{s}$ configuration. These conspicuously OZI rule violation reactions are of considerably theoritical interest, since the production of flavor mixing or exotic (glueballs, hybrids) violates the OZI rule , for example, the processes for glueball production are $\sqrt{\text{OZI}}$

suppressed; and OZI breaking can be linked with the nucleon structure, in particular the problem of the intrinsic $s\bar{s}$ in nucleons; it also can help us to understand the production and decay mechanism of the final hadrons.

Two different theoritical approaches have been used to interpret the observation[16, 17]. One is based on the $\omega \sim \phi$ mixing and the higher order processes beyond tree level[16], the other assumes that there exists intrinsic $s\bar{s}$ in nucleons[17]. In the naive constituent quark model, the neucleons only contain just two kinds of quarks u and d. It describe a good general picture of nucleons at large distance, but at shorter distance, probes reveal more constituents, including a sea of $q\bar{q}$ (q=u,d,s, even c) pairs and gluons. Evidence indicates that there are $s\bar{s}$ pairs in nucleons even at large distance[18] from polarized deep inelastic scattering experiments. If the intrinsic $s\bar{s}$ components in nucleons was introduced, naturally, it can explain the strongly enchanced ϕ production. But the situation is **quite different** for charmonia decays involving ϕ and ω final states.

Another interpretation considers the $\omega \sim \phi$-mixing and higher order contributions[16]. In massless QCD, the hadrons composed of u, d, s quarks would form SU(3) multiplets, but actually s quark is much heavier than u and d quarks, and the SU(3) flavor symmetry is broken. Particularly, the physical states ω and ϕ are the superpositions of the SU(3) singlet ω_1 and octet ω_8 states, cf Fig. 4.

$$\begin{pmatrix} \phi \\ \omega \end{pmatrix} = \begin{pmatrix} cos\theta & -sin\theta \\ sin\theta & cos\theta \end{pmatrix} \begin{pmatrix} \omega_8 \\ \omega_1 \end{pmatrix}$$

where

$$\omega_1 = \frac{1}{\sqrt{3}}(u\bar{u} + d\bar{d} + s\bar{s}) = \sqrt{\frac{2}{3}}q\bar{q} + \sqrt{\frac{1}{3}}s\bar{s}$$

$$\omega_8 = \frac{1}{\sqrt{6}}(u\bar{u} + d\bar{d} - 2s\bar{s}) = \sqrt{\frac{1}{3}}q\bar{q} - \sqrt{\frac{2}{3}}s\bar{s}$$

and $q\bar{q} = \sqrt{\frac{1}{2}}(u\bar{u} + d\bar{d})$. The so-called ideal mixing corresponds to a complete decoupling of the $s\bar{s}$ and $q\bar{q}$:

$$\theta_i = arctg\sqrt{\frac{1}{2}} = 35.3^0$$

then

$$\phi = s\bar{s}$$
$$\omega = \sqrt{\tfrac{1}{2}}(u\bar{u} + d\bar{d})$$

while the mixing angle determined from the ratio $R = \Gamma(\phi \to e^+e^-)/\Gamma(\omega \to e^+e^-,)$ which is in principle sensitive to the $\omega \sim \phi$ mixing [19],

$$\theta = 37.1^0$$

Gell-Man-Okubo mass formula gives

$$\theta \approx 39^0.$$

Therefore, based on the assumption that the couplings of the ϕ and $f(1525)$ to nonstrange hadrons are entirely due to a nonstrange admixture in the wave function which was described by a single mixing angle departing from the ideal mixing in each case, the phenomenologically "universal mixing model" gave[20]:

$$\begin{aligned}\frac{\sigma(\phi X)}{\sigma(\omega X)} &= tg^2\delta\theta_V = tg^2(\theta_i - \theta) \approx (\theta_i - \theta)^2 \\ &= (1 \sim 4.2) \times 10^{-3}.\end{aligned}$$

Similarly for tensors $f_2'(1525)/f_2(1270)$,

$$\frac{\sigma(f_2' X)}{\sigma(f_2 X)} = tg^2\delta\theta_T$$

Since $\theta \neq \theta_i$, so the OZI forbidden processes involving the ϕ production can proceed via the $s\bar{s} \sim q\bar{q}$ mixing, but the relative cross section $tg^2\delta\theta$ is of 10^{-3} order.

From the J/ψ hadronic decays into $\{\omega, \phi\}X$, it was found that the hadronic decays are also highly selective regarding the flavor of the final state X, as one expects a quark correlation between the vector meson and the recoiling system X. However the observed final states arising from the two gluon system in radiative decays are flavor independent. One expects that the singly disconnected diagram 3a dominates over the doubly disconnected one 3b, as confirmed from the large observed value [12] for $Br(J/\psi \to \omega f_2)/Br(J/\psi \to \omega f_2') > 50$. Since the vector nonet is almost ideally mixed, the ϕ tags recoiling states with strangeness, while the ω is expected to go with non-strangeness systems.

When comparing the hadronic decays of the J/ψ, it was shown that the SU(3) symmetry is broken in a non-negligible way. This breaking manefests itself in a suppression of the final states with strange quarks, thus leading the smaller rates for ϕX relative to ωX channels. This was systematically studied in the J/ψ decays into the $1^{--}0^{-+}$ vector-pseudoscalar modes [21].

The branching ratio $R = \Gamma(J/\psi \to \phi\pi^+\pi^-)/\Gamma(J/\psi \to \omega\pi^+\pi^-) = 0.11 \pm 0.02$ [12] is too large with respect to the naive phenomenogical $\omega \sim \phi$ mixing model. As it was pointed out that the contribution of higher order processes via intermediate states containing both $s\bar{s}$ and u or d quarks (including final state interaction) can enhance the ϕ production in Ref. [16]; Because of the flavor mixing, the OZI forbidden transition can proceed via the two-step process by exchanging intermediate states in which each step is OZI allowed, that is, the transition via intermediate states with mixed flavors can be produced via one component and decay via another. Extensive investigations have shown that the nonet symmetry of the intermediate states and exchange degeneracy which appear automatically in the duality description of hadron processes lead to destructive interference and the cancellations between the contributions from different intermediate states and play a crucial role in suppressing these OZI-violating higher order transitions, i.e, the contributions from the hadronic loops are negligible, the OZI rule preserves. It has been proved that the OZI rule can hold only in the nonet symmetry limit when the contributing intermediate states can be expressed in a basis of physical quarkonium states with a single flavor. Once the nonet symmetry is broken, the physical states are always flavor mixtures, the cancellation does not occur, the hadronic loop diagrams are large, and the interference effects between different intermediate states are of importance, the propagators of such intermediate mixed states break the OZI rule [22]. Of particular interest is the $f_0(980)$ scalar meson which has dominant strange component and a $\pi\pi$ decay mode [23]. The $\phi\pi^+\pi^-$ final state in J/ψ decay has been found to be dominated by the ϕf_0 configuration [12]. Since there are large mass splittings in the f_0 scalar nonet and f_0 is near $K\bar{K}$ threshold, the cancellation mechanism breaks down, leading to very large OZI violation loop effects which are exepected to manifest themselves as large shifts in the masses and large mixing of $s\bar{s}$ and $u\bar{u}+d\bar{d}$ of scalar nonet large OZI violation. But this explanation introduces many parameters that have to be determined by experiments, and it is phenomenological and has weak predictability unless the experimental results come out.

A full description of the OZI rule is hopefully be obtained eventually from QCD. However, at present stage QCD has proved to be useful only in the simplest cases: namely the decays of heavy quarkonium vector mesons into light quark final states. In this case the dominant diagram for the OZI forbidden processes, the annihilation of the massively heavy quark-antiquark pair into three high-momentum gluons has been successfully treated by perturbative QCD [11], meanwhile, it has been pointed out that the amplitudes from soft gluons are of higher order and rather small [24]. Therefore for charmonia decay into light flavor hadrons, a rough estimate gave [25]:

$$\frac{\Gamma(J/\psi \to \phi\pi^+\pi^-)}{\Gamma(J/\psi \to \omega\pi^+\pi^-)} \sim 0.14$$

with $\alpha_s(m_\phi^2) = 0.55$ and neglecting the small phase-space difference and the wave function discrepancy in the binding of ω and ϕ, and $\Gamma(J/\psi \to \phi K^+K^-)$ and $\Gamma(J/\psi \to \omega K^+K^-)$ are comparable. The similar results can be drawn for $\Psi(2S)$ decays, but it gave:

$$\frac{\Gamma(\psi' \to \phi\pi^+\pi^-)}{\Gamma(\psi' \to \omega\pi^+\pi^-)} > \frac{\Gamma(J/\psi \to \phi\pi^+\pi^-)}{\Gamma(J/\psi \to \omega\pi^+\pi^-)}$$

since the small difference of α_s at $\sqrt{s} = m_J/\psi$ and $m_{\psi'}$ and the wave function of J/ψ and ψ' at the origin. As mentioned in Ref.[26], since the $\phi\pi^+\pi^-$ is dominant as a ϕf_0

configuration, the mixing effects in 0^{++} nonet will soften the OZI suppression in the ratios $\Gamma(\psi(nS) \to \phi\pi^+\pi^-)/\Gamma(\psi(nS) \to \omega\pi^+\pi^-)$.

Of course, the OZI rule is evidently not absolute, it is a good approximation for a large number of strong interaction processess. Attempts have been made to understand the origin of the OZI rule within the framework of $N_C = 3$ QCD [27], it has been shown that the OZI rule should work well for heavy flavors [11]. But it is established that the OZI rule emerges as a rigorour consequence of the application of the large N_C limit to QCD. It has been proved that, in the large N_C limit, the transition amplitude of the connected quark line diagram corresponding to Fig. 2a is ${N_C}^{-1/2}$ whereas it is ${N_C}^{-3/2}$ in the case of the disconnected quark line diagram of Fig. 2b. From another aspect, the large N_C estimates clearly tell us that the relative decay widths of the OZI forbidden processess and the allowed ones is ${N_C}^{-2}$. relative decay widths of the DOZI processes (cf. Fig. 3b) to those of the SOZI processes (cf. Fig. 3a) is also about ${N_C}^{-2}$. The OZI rule is rigorous in the $N_C \to \infty$ limit, but we have no way to estimate the degree of accuracy of the OZI rule for finite $N_C = 3$, the violation of the OZI rule may occur.

In brief, the naive phenomenologically universal $\omega \sim \phi$ mixing model does not seem to properly describe some OZI forbidden processess, especially the DOZI processes such as $J/\psi \to \phi K^+K^-$. perturbative QCD gives quantitative approximation for heavy quarkonium hadronic decays, and the large N_C estimates gives a general quantitative description of the OZI rule.

1.3 Main Motivations

As mentioned above, because of the different situation between the ϕ and ω production from charmonium decays and from nucleon or meson-nucleon collisions, so search for the OZI or DOZI suppression violation with respect to the $\omega \sim \phi$ mixing model in $\Psi(2S)$ decays involving ϕ and ω are of great importance and it will help us to understand the $\Psi(2S)$ hadronic decay mechanism, it is one goal of this work. Moreover, in contrast to the numerous decay modes of J/ψ, much fewer decay modes of $\Psi(2S)$ are available now [12], so the study of the decay modes of $Psi(2S)$ are possible because of much larger data samples collected at BES. The decay channels to be investigated are $\Psi(2S) \to (\omega,\, \phi) + (\pi^+\pi^-, K^+K^-, p\bar{p})$, then ω decays into $\pi^+\pi^-\pi^0 \to \pi^+\pi^-\gamma\gamma$ and ϕ into K^+K^-, by the way the decays of $\Psi(2S) \to \pi^+\pi^-\pi^0 p\bar{p}$ and $\eta\pi^+\pi^-p\bar{p}$ with (π^0, η) decays to $\gamma\gamma$ and $\Psi(2S) \to \phi f_0$ with $\phi \to K^+K^-$ and $f_0 \to \pi^+\pi^-$are analyzed. At the same time, the first measurements of the branching ratios of the corresponding decay channels and the study of SU(3) flavor symmetry breaking are to be presented, and also the QCD "15%" rule is tested.

2 Study of $\Psi(2S)$ decay modes involving ω and ϕ

2.1 Data Sample

Using the $(3.79 \pm 0.31) \cdot 10^6$ $\Psi(2S)$ data taken from 1993 to 1995 at BES detector, I analyse the $\Psi(2S)$ three-body decay final states involving ω and ϕ, the final states are 4-prongs for the events involving ϕ and 4-prongs plus 2γ for those involving ω. Applying HOWL plus angular distributions event generators, the MC samples are generated to study the acceptance and the backgrounds after passing through the same analysis programs. The three-body decays of $\Psi(2S)$ and ω are generated by HOWL, and the vector mesons decays to two pseudoscalar mesons are generated by the distributions of $sin^2\theta$.

The decay branching ratios from PDG[9, 12] used for analyses are:

$Br(\phi \rightarrow K^+K^-) = (49.1 \pm 0.8)\%$, $Br(\pi^0 \rightarrow 2\gamma) = (98.798 \pm 0.032)\%$,
$Br(f_0 \rightarrow \pi^+\pi^-) = (78.1 \pm 2.4)\%$, $Br(\eta \rightarrow 2\gamma) = (39.21 \pm 0.34)\%$,
$Br(\omega \rightarrow \pi^+\pi^-\pi^0) = (88.8 \pm 0.7)\%$, $Br(J/\psi \rightarrow \omega\pi^+\pi^-) = (7.2 \pm 1.0) \cdot 10^{-3}$,
$Br(J/\psi \rightarrow \phi\pi^+\pi^-) = (8.0 \pm 1.2) \cdot 10^{-4}$, $Br(J/\psi \rightarrow \phi f_0) = (3.2 \pm 0.9) \cdot 10^{-4}$,
$Br(J/\psi \rightarrow \phi p\bar{p}) = (4.5 \pm 1.5) \cdot 10^{-5}$, $Br(J/\psi \rightarrow \pi^0\pi^+\pi^- p\bar{p}) = (2.3 \pm 0.9) \cdot 10^{-3}$,
$Br(J/\psi \rightarrow \omega p\bar{p}) = (1.3 \pm 0.25) \cdot 10^{-3}$, $Br(J/\psi \rightarrow \omega K^+K^-) = (7.4 \pm 0.7 \pm 2.3) \cdot 10^{-4}$,
$Br(J/\psi \rightarrow \phi K^+K^-) = (8.3 \pm 0.3 \pm 1.3) \cdot 10^{-4}$, $Br(J/\psi \rightarrow \eta\pi^+\pi^- p\bar{p}) = No\ PDG\ data.$

Note: Actually, the branching ratio $Br(f_0 \rightarrow \pi\pi)$ from PDG refers to $Br(f_0 \rightarrow \pi^+\pi^-)$, not including f_0 decays into $\pi^0\pi^0$.

The magnetic field shift correction, dE/dX correction, TOF correction, vertex correction and neutral track error matrix corrections are applied into analyses, of course the magnetic field shift correction is done only for DATA, not for MC samples. Correspondingly modify some subroutines from BES Library to avoid duplicate corrections.

2.2 Method

In order to get better particle separation, combine kinematic fit and dE/dX information for particle identification. For different particle assignments, the smallest

$$\chi^2 = \chi^2_{fit} + \sum_i (\chi^2_{s_i dE/dX}) \tag{1}$$

is selected as the best one, but don't use bad TOF information, meanwhile, analysis indicates that hardly any difference is made even without TOF information, where χ^2_{fit} is the χ square for the kinematic fit , and

$$\chi_{s_i dE/dX} = \frac{(dE/dX)^{meas} - (dE/dX)^{th}_i}{\sigma_i^{(dE/dX)}}$$

is the measured dE/dX pulse height $(dE/dX)^{meas}$ deviation of the i^{th} particle from the theoritical expectation $(dE/dX)_i^{th}$ as a certain particle hypothesis, $\sigma_i^{(dE/dX)}$ is the resolution of dE/dX pulse height, and summation over all final charged particles with good reconstructed tracks.

2.3 Breit-Wigner Fits for the Resonances

The mass spectra of resonances are given as foldproduct of a Breit-Wigner formula and a gaussian function of mass resolution plus a polynomial background (I only use the first 3-polynomials):

$$f(m) = \sum_i a_i \int dx \frac{(\Gamma_i/2)^2}{(x-m_i)^2 + (\Gamma_i/2)^2} \cdot \frac{1}{\sqrt{2\pi}\sigma_i} \cdot e^{-\frac{(x-m)^2}{2\sigma_i^2}} + (1 - \sum_i a_i) bgs(m)$$

the full fit function is normalized while fitting, where i is the number of the resonances, m_i and Γ_i are the mass and width of resonance i, σ_i is the corresponding mass resolution, a_i stands for the ratio of the area of resonance i to the full area in the fit regions, $bgs(m)$ used here is only a 3-polynomial $(p_0 + p_1 m + p_2 m^2)$. Use the CERN Library package MINUIT[28] to minimize a above-given function formula from BES Library and the Minuit processor MIGRAD or MINOS to produce an error matrix and obtain the above fit parameters through the method of maximum likelihood function.

The unbinned B-W fits are done for my analyses.

2.4 Event Selection

2.4.1 General Cuts

The BES detector has been described elsewhere[29] in detail. The following are event selection criteria.

- Charged tracks: events with good run, four charged tracks of good helix track fit (Mfit=2) for **EACH** track, and zero net charge ($Netchrgs = 0$) are selected, each track lying in polar angle regions $|\cos\theta| < 0.8$, and the event vertex in the regions $V_{xy} = \sqrt{V_x^2 + V_y^2} < 1.5cm$ and $|V_z| < 15cm$, and $|\chi_s| < 3$ for **EACH** track.

- isolated photon: neutral clusters hit Barrel Shower Counter (BSC) at least 2 layers, $N_{lays} \geq 2$ and do not hit the central ribbon range ($|Z_{sc}| < 4cm$). In order to remove radiative photons from charged particles, require the angle between the photons and the charged particles satisfy $|cos\theta_{\gamma\sim chrg}| < 0.96$. And the angle between the direction of the neutral track hiting on BSC and its developing direction in BSC satisfy $|cos\theta_{\gamma\sim dev}| >$

0.8. The energy of the photons after the kinematic fit should be greater than 60MeV, $E_{\gamma-fit} > 60MeV$. And the number of neutral clusters is not limited. Because of bad energy resolution of BSC ($\sigma_E/E = 25\%/\sqrt{E}$), only the above cuts are used, it is a bit loose, but kinematic fit will work to get good photons.

- electron: there are a few eletron backgrounds from $\Psi(2S) \to \eta J/\psi \to \pi^+\pi^-\pi^0 J/\psi \to \pi^+\pi^-\pi^0 e^+e^-$ decays. The charged tracks with $|\chi_{se}|$ less than 3 ($|\chi_{se}| < 3$), and the ratios of their energy deposit E_{sc} in BSC to their momenta $p_{1,2}$ satisfying $\frac{E_{sc1,2}}{p_{1,2}} > 1$, or

$$(\frac{E_{sc1}}{p_1} - 1)^2 + (\frac{E_{sc2}}{p_2} - 1)^2 \leq 0.36.$$

  are identified as electrons, and the events with any identified electron should be removed.

- muon: there are a few muon backgrounds from $\Psi(2S) \to \eta J/\psi \to \pi^+\pi^-\pi^0 J/\psi \to \pi^+\pi^-\pi^0\mu^+\mu^-$ decays. We identify the charged particles as muons if they hit on μ-counter, and lie in the μ-counter coverage ($|cos\theta| < 0.6$), and their total hit layers in μ-counter are not less than 3 ($\sum N_{lays} \geq 3$), the events will be rejected.

- J/ψ background: there are large J/ψ backgrounds, the event with recoil mass

$$m_{recoil} = \sqrt{(E_{cm} - E_1 - E_2)^2 - (\vec{\mathbf{p}}_\mathbf{1} + \vec{\mathbf{p}}_\mathbf{2})^2}$$

  of any oppositely-charged particle pair with the momentum of each particle less than 0.6GeV is identified as J/ψ if $m_{recoil} \in (3.05, 3.15)GeV$. Removing $\pi^+\pi^- J/\psi$, $\pi^+\pi^- e^+e^-$, $\pi^+\pi^-\mu^+\mu^-$ events will almost reject all J/ψ background.

- 5-C fit: in order to get better ω mass resolution, an extra constraint with two photons forming a resonance π^0 is applied into the kinematic fit, that is, 5-C fit is done for the processes involving ω, while 4-C fit for the processes without photons. It is unquestionably reasonable, because the π^0 decay width is negligible compared to its mass resolution at BES.

- probability cut: the χ^2-probability for kinematic fit

$$CL(fit) = prob(\chi^2_{fit}, ndf_{fit})$$

  and the χ^2-probability of dE/dX for all charged particles

$$CL(dE/dX) = prob(\sum_i \chi^2_{s_i dE/dX}, ndf_{dE/dX})$$

  are both required to be greater than 1%, where ndf's are the corresponding number of degree of freedom for kinematic fit and dE/dX. Within my analyses, ndf_{fit} equals 4 for 4-C fit, 5 for 5-C fit. and $ndf_{dE/dX}$ equals 4.

Criteria for the Specific Channals

2.4.2 $\Psi(2S) \rightarrow \omega\pi^+\pi^-$ with $\omega \rightarrow \pi^+\pi^-\pi^0 \rightarrow \gamma\gamma\pi^+\pi^-$, low background from ωK^+K^-

The events satisfying the general cuts(cf Sec. 2.4.1) are kinematically $5C - 2\gamma$ fitted for $\gamma\gamma\pi^+\pi^-\pi^+\pi^-$ with all pairs of photon candidates forming π^0. The pair with the highest probability of fit are selected and it is also required to be greater than 1%, as mentioned above among the general cuts. Since all particles are pions, we can only compare the probability of fit to select the events. The background ωK^+K^- is rejected if the events with the probability of kinematic fit and that of dE/dX greater than 0.01, and the combined probability of kinematic fit plus dE/dX greater than that of $\omega\pi^+\pi^-$. Briefly, the cuts are listed as following:

- $CL(5C)_{\omega\pi^+\pi^-} \geq 0.01$, $CL(dE/dX)_{chrgs} \geq 0.01$, $E^{fit}_{\gamma min} > 60MeV$,
- reject ωK^+K^-, ωK^+K^- is identified if CL(5C)$_{\omega K^+K^-} \geq 0.01$, CL(dE/dX)$_{\omega K^+K^-} \geq 0.01$, and CL(5C+dE/dX)$_{\omega K^+K^-} >$ CL(5C+dE/dX)$_{\omega\pi^+\pi^-}$

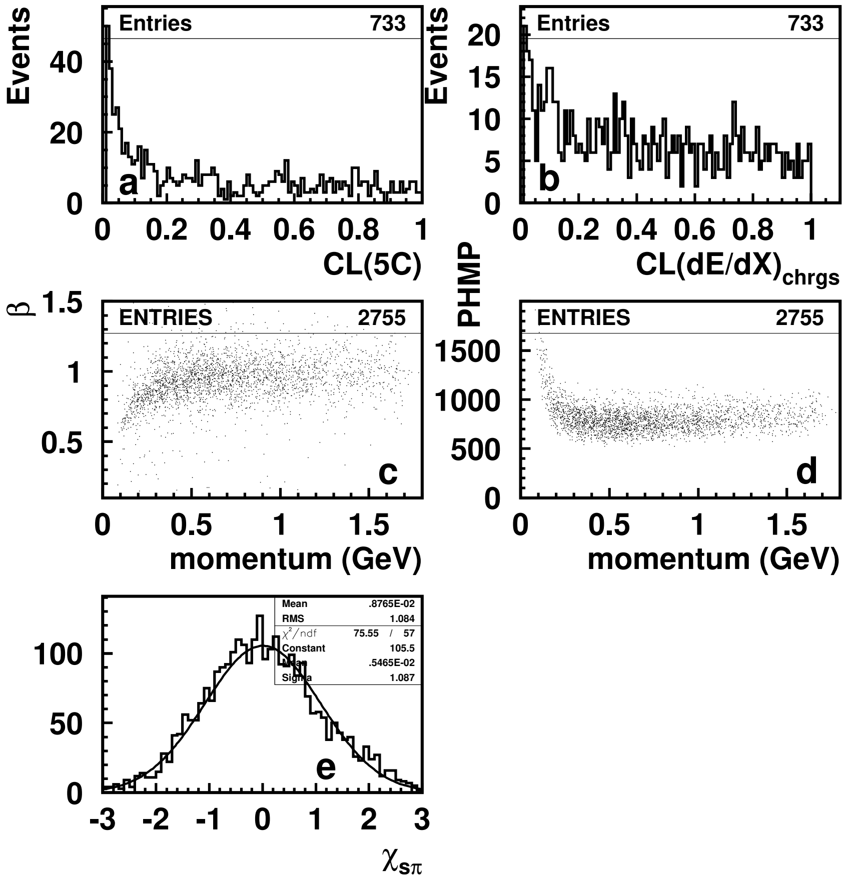

Figure 5: $\Psi(2S) \rightarrow \omega\pi^+\pi^-$, the distributions of the probability of 5-C fit(a) and that of the dE/dX (b) of all charged particles; TOF β (c) and the dE/dX phulse height (d) v.s. momenta, (e) χ_{s_π} distribution of the selected charged pions.

Fig. 5(a,b) repectively show the probability of the 5-C kinematic fit and dE/dX, the β and dE/dX pulse height of particles versus their momenta are depicted in Fig. 5(c,d). From (c,d), we can conclude that dE/dX information are much better than TOF when used to identify paritcles on account of the better resolution of dE/dX than that of TOF. Fig 5e shows the dE/dX particle separation of the selected pions χ_{s_π} distribution, it is quite good (0,1.0) Gaussian. These figures reflect the analysis is reliable.

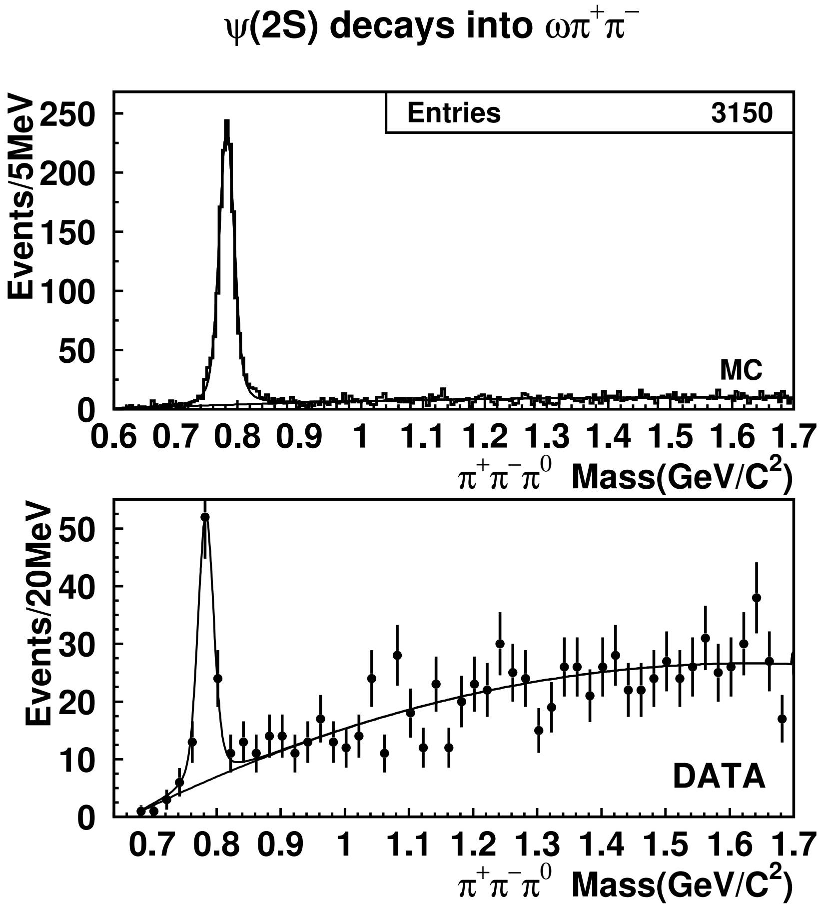


```
================================================================================
I                      Summary Of BWFIT Results                                I
================================================================================
Histogram ID=     1  UnBinned Breit-Wigner Fit using 1028 Points
Fit Parameters:Npoly=   3 Nbw=   1 Namp=   0 Range=       .680 To      1.700
Hist. Chisq =       51.83 for    4 params &  46 DF.
Chisquare Probability =  25.69%. Mean and S.D. for pulls:    -.0673    1.0059
Likelihood ratio and probability             :     22.050        99.89%
Final Value of Log Likelihood                :       -72.92
Error Correspond to a Function Chage         :      .50
Phase Space limits for tails corrections     :       .280GEV     2.817GEV
Breit-Wigner efficiency correction factors   :      .985
Include Breit-Wigner tails outside fit region :        .997
Efficiency-corrected events in fit region    :     1028.[average eff. :1.000]
---THE FITTED VALUES AND ERRORS OF THE PARAMETERS:---
leg1    Value :  .68869    Error(Cov,-/+):    .499E-01 -.501E-01  .497E-01
leg2    Value : -.26491    Error(Cov,-/+):    .571E-01 -.554E-01  .590E-01
Rate    Value :  .77102E-01Error(Cov,-/+):    .994E-02 -.967E-02  .102E-01
RESL    Value :  .10330E-01Error(Cov,-/+):    .000E+00 -.186E-02  .185E-02
GAMA    Value :  .84300E-02Error(Cov,-/+):    .000E+00  .000E+00  .000E+00
MASS    Value :  .78312    Error(Cov,-/+):    .185E-02  .000E+00  .000E+00
```

Figure 6: unbinned B-W fit for $\Psi(2S) \to \omega\pi^+\pi^-$, the upper for MC, the lower for DATA.

Fig. 6 diagram the unbinned B-W fit for $\pi^+\pi^-\pi^0$ invariant mass(4 entries per event), the upper for MC simulation, the lower for DATA. An obvious ω signal over the combinational background can be seen, the fitted results will be listed with others in Table 3 later.

2.4.3 $\Psi(2S) \rightarrow \phi\pi^+\pi^-$, backgrounds from $\Psi(2S) \rightarrow K^+K^-K^+K^-$, $\pi^+\pi^-\pi^+\pi^-$

As describe in Sec. 2.2, the kinematic fit for $K^+K^-\pi^+\pi^-$ is combined with the dE/dX information. The events with the smallest total χ^2 (cf Eq. 1) of fit and dE/dX for different π/k hypotheses are selected, and also required the 4-C fit probability and all charged particle dE/dX probabilty are above 1%. To reject background, the combined probability of fit plus dE/dX should be greater than those of $\Psi(2S) \rightarrow K^+K^-K^+K^-, \pi^+\pi^-\pi^+\pi^-$. Of course, the events must pass the general cuts (see Sec. 2.4.1). For brevity, the cuts are as following:

- $\mathrm{CL}(4\mathrm{C})_{\pi^+\pi^-K^+K^-} \geq 0.01$, $\mathrm{CL}(\mathrm{dE/dX})_{chrgs} \geq 0.01$,
- $CL(4C + dE/dX)_{\pi^+\pi^-K^+K^-} > CL(4C + dE/dX)_{K^+K^-K^+K^-,\pi^+\pi^-\pi^+\pi^-}$

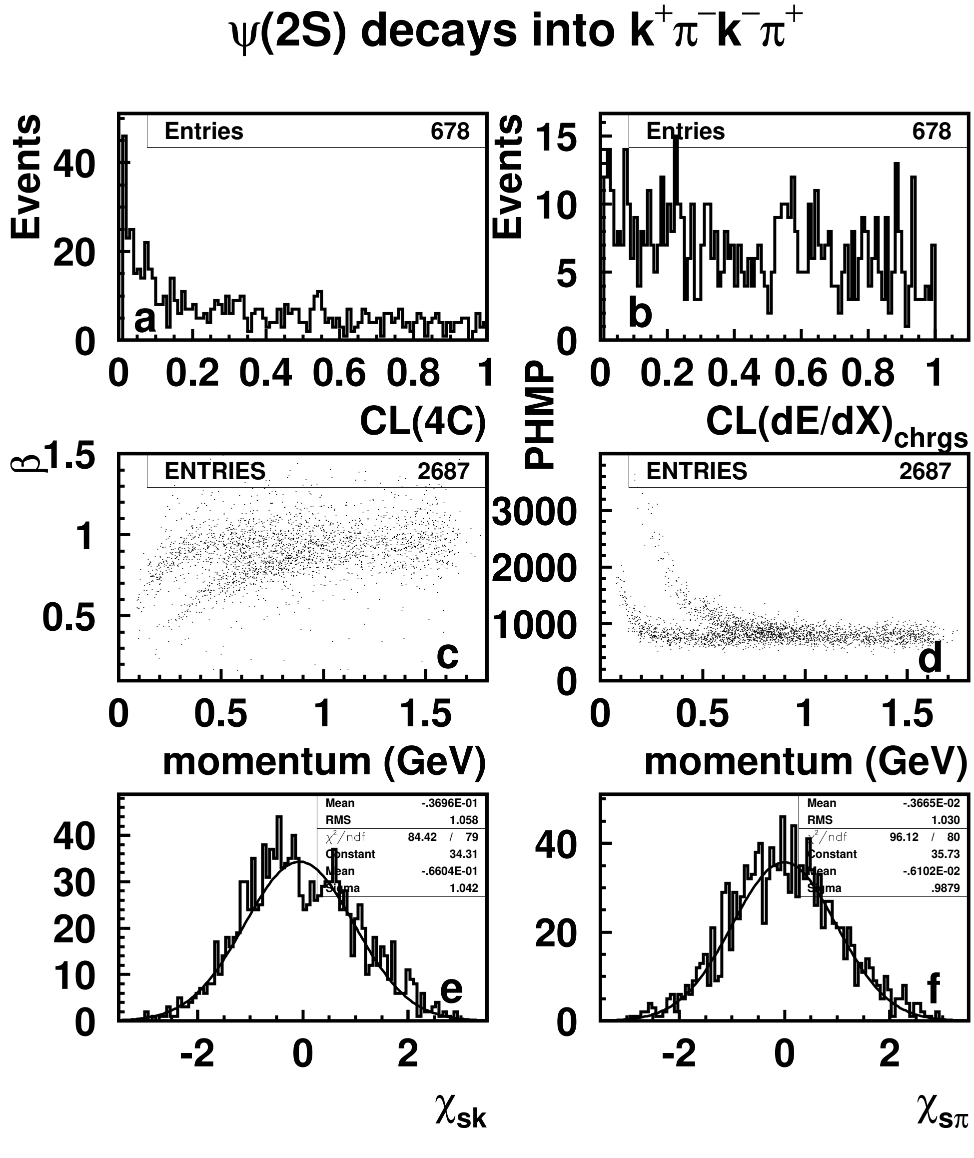

Figure 7: $\Psi(2S) \rightarrow \phi\pi^+\pi^-$, The distributions of the probability of 4-C fit (a) and dE/dX (b), TOF β (c) and dE/dX pulse height (d) v.s particle momenta, (e,f) χ_{s_K}, χ_{s_π} distributions.

The distributions of the probability of 4-C fit and dE/dX of all charged particle are presented in Fig. 7 for the events surviving the above cuts and the general cuts, cf Sec. 2.4.1.

The distributions of the probability are almost flat, it confirms our method (Sec. 2.2) is unquestionable. From Fig. 7(c,d), once again, it can be seen that dE/dX information are much better than TOF if used to seperate different kinds of particles. Fig. 7(e,f) represent the dE/dX particle separation χ_{s_K} and χ_{s_π} of the selected kaons and pions, they are both good (0,1) Gaussian. It means that our method is reliable.

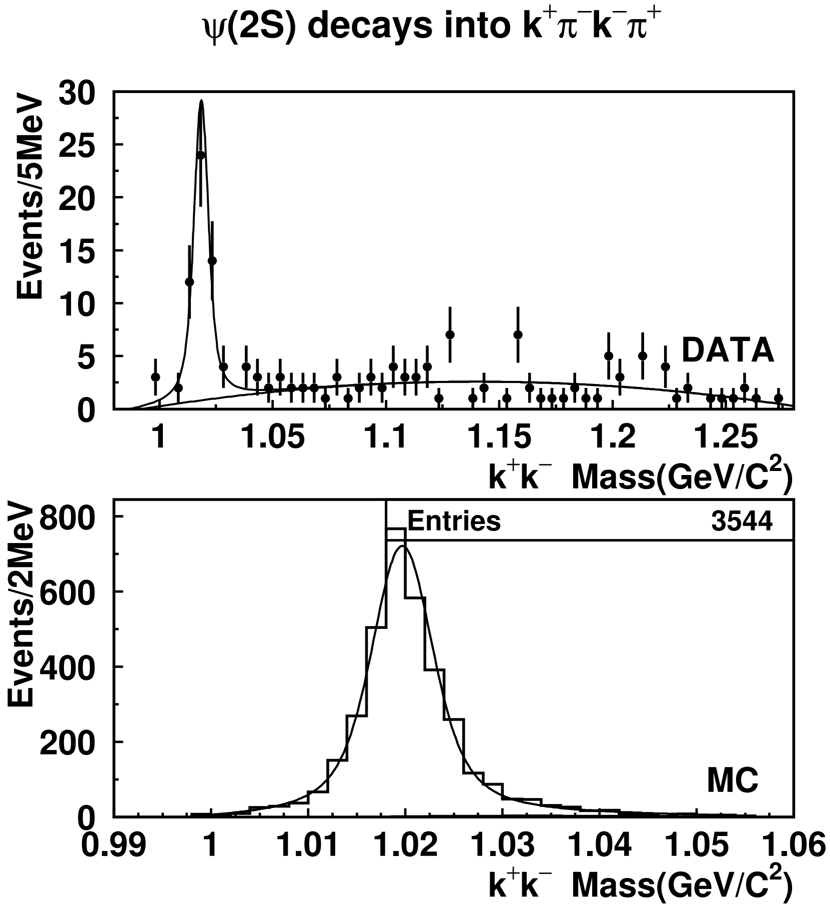


```
==============================================================================
I                    Summary Of BWFIT Results                               I
==============================================================================
Histogram ID=     1  UnBinned Breit-Wigner Fit using  158 Points
Fit Parameters:Npoly=   3 Nbw=   1 Namp=   0 Range=       .980 To      1.280
Hist. Chisq =      60.50 for   4 params &  48 DF.
Chisquare Probability =  10.64%. Mean and S.D. for pulls:     .0135    1.0683
Likelihood ratio and probability            :     61.192         9.57%
Final Value of Log Likelihood               :      -265.76
Error Correspond to a Function Chage        :      .50
Phase Space limits for tails corrections    :       .280GEV     2.817GEV
Breit-Wigner efficiency correction factors  :      .979
Include Breit-Wigner tails outside fit region :       .999
Efficiency-corrected events in fit region   :      158.[average eff. :1.000]
---THE FITTED VALUES AND ERRORS OF THE PARAMETERS:---
leg1    Value :  .21910    Error(Cov,-/+):    .144     -.149      .141
leg2    Value : -1.0581    Error(Cov,-/+):    .180     -.161      .197
Rate    Value :  .36349    Error(Cov,-/+):    .455E-01 -.448E-01  .462E-01
RESL    Value :  .21000E-02Error(Cov,-/+):    .000E+00 -.566E-03  .570E-03
GAMA    Value :  .44300E-02Error(Cov,-/+):    .000E+00  .000E+00  .000E+00
MASS    Value :  1.0185    Error(Cov,-/+):    .567E-03  .000E+00  .000E+00
```

Figure 8: $\Psi(2S) \to \phi\pi^+\pi^-$, B-W fit for DATA(the upper) and MC(the lower).

The unbinned B-W fit results for ϕ signals are shown in Fig. 8, and will be listed in Table 3 later.

2.4.4 $\Psi(2S) \to \phi f_0(980)$, backgrounds from $\Psi(2S) \to K^+K^-K^+K^-$, $\pi^+\pi^-\pi^+\pi^-$

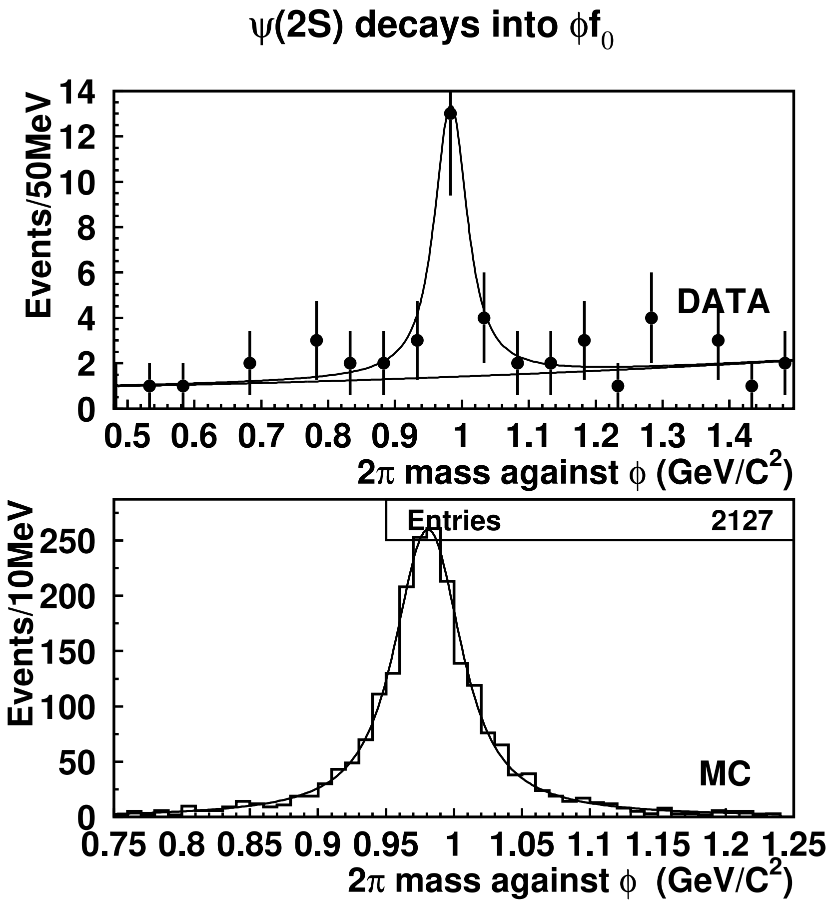


```
==============================================================================
I                      Summary Of BWFIT Results                              I
==============================================================================
Histogram ID=     1  UnBinned Breit-Wigner Fit using    50 Points
Fit Parameters:Npoly=   3 Nbw=   1 Namp=   0 Range=       .480 To      1.500
Hist. Chisq =      12.33 for   4 params &  15 DF.
Chisquare Probability =  65.42%. Mean and S.D. for pulls:    -.0329     .7844
Likelihood ratio and probability             :     14.115        51.68%
Final Value of Log Likelihood                :       -14.36
Error Correspond to a Function Chage         :      .50
Phase Space limits for tails corrections     :       .280GEV     2.817GEV
Breit-Wigner efficiency correction factors   :      .969
Include Breit-Wigner tails outside fit region :        .984
Efficiency-corrected events in fit region    :       50.[average eff. :1.000]
---THE FITTED VALUES AND ERRORS OF THE PARAMETERS:---
leg1    Value :  .39117    Error(Cov,-/+):    .336     -.331      .342
leg2    Value :  .68037E-01Error(Cov,-/+):    .478     -.430      .525
Rate    Value :  .40631    Error(Cov,-/+):    .103     -.101      .104
RESL    Value :  .94000E-02Error(Cov,-/+):    .000E+00 -.807E-02  .818E-02
GAMA    Value :  .50000E-01Error(Cov,-/+):    .000E+00  .000E+00  .000E+00
MASS    Value :  .98342    Error(Cov,-/+):    .805E-02  .000E+00  .000E+00
```

Figure 9: $\Psi(2S) \to \phi f_0$, the unbinned B-W fit for DATA (the upper) and MC (the lower).

As a controversial candidate of exotic states, scalar meson $f_0(980)$ with $J^{PC} = 0^{++}$, is sepecially intriguing for both theories and experiments[30]. Since it is near $k\bar{k}$ threshold, it can decay to both $\pi\pi$ and $k\bar{k}$, $f_0(980)$ and $a_0(980)$ almost degenerate in mass (although their decay channels are not same, but they can couple via mixing), $f_0(980)$ has always been considered ciritical. $f_0(980)$ and $a_0(980)$ play a peculiar role in the dynamics of quark confinement[31]. So the structure of $f_0(980)$ is of great importance to distinguish the different interpretations. I analyse the $f_0(980)$ production in $\Psi(2S)$ decays. The cuts are same as those for $\Psi(2S) \to \phi\pi^+\pi^-$, see Sec. 2.4.3, an additional cut requires K^+K^- invariant mass $m_{K^+K^-} \in (1.0, 1.04)$, the unbinned B-W fit for $\pi^+\pi^-$ recoil mass against ϕ are shown in Fig. 9. From the figure, there are lower backgrounds for $\Psi(2S) \to \phi f_0$ production in $\Psi(2S)$ decays than in J/ψ[32]. It's better to study f_0 production in $\Psi(2S)$ decays, but we only have low statistic data sample. The results are to be listed in Table 3.

2.4.5 $\Psi(2S) \to \omega K^+K^-$, main background from $\Psi(2S) \to \omega\pi^+\pi^-$

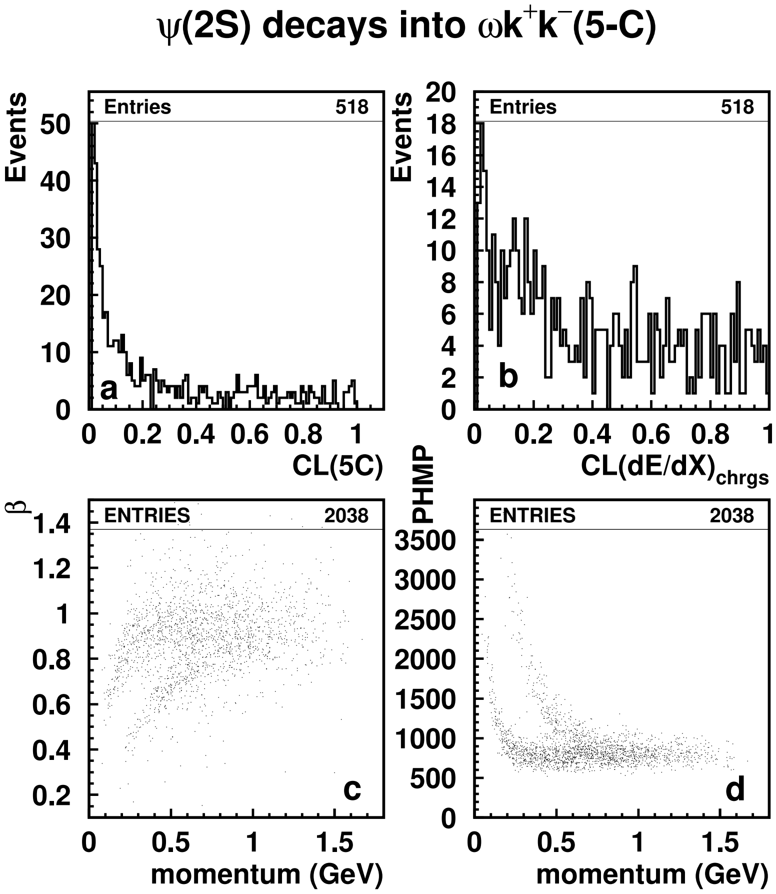

Figure 10: $\Psi(2S) \to \omega K^+K^-$, same as $\Psi(2S) \to \phi\pi^+\pi^-$, the distributions of probability of 5-C fit (a) and that of dE/dX (b), and TOF β (c) and dE/dX phulse height (d) v.s particle momenta. Similar χ_{s_π}, χ_{s_K} distributions as Fig. 7(e,f) (not presented here).

With $\omega \to \pi^+\pi^-\pi^0 \to \gamma\gamma\pi^+\pi^-$, after general cuts (see Sec. 2.4.1), 5C-2γ kinematic fit for $\gamma\gamma K^+K^-\pi^+\pi^-$ is done with all pairs of photon candidates forming a resonance π^0 and loop over different π/k hypotheses for all charged tracks, the kinematic fit is combined with dE/dX information, events with the lowest total $\chi^2 = \chi^2_{5C-fit} + \sum_i(\chi^2_{s_i dE/dX})$ are selected, and also the probability of 5-C fit and that of dE/dX are required to be above 1%. To exclude background $\omega\pi^+\pi^-$, $\omega\pi^+\pi^-$ is identified if the probability of 5-C fit and that of dE/dX of all charged particle are greater than 1%, and also the combined probability of 5-C fit plus dE/dX is required to be greater than that of ωK^+K^-. The cuts are briefly listed here:

- $CL(5C)_{\omega K^+K^-} \geq 0.01$, $CL(dE/dX)_{chrgs} \geq 0.01$, $E^{fit}_{\gamma min} > 60MeV$,
- reject $\omega\pi^+\pi^-$, $\omega\pi^+\pi^-$ is identified if $\mathrm{CL(5C)}_{\omega\pi^+\pi^-} \geq 0.01$, $\mathrm{CL(dE/dX)}_{\omega\pi^+\pi^-} \geq 0.01$, and $\mathrm{CL(5C+dE/dX)}_{\omega\pi^+\pi^-} > \mathrm{CL(5C+dE/dX)}_{\omega K^+K^-}$

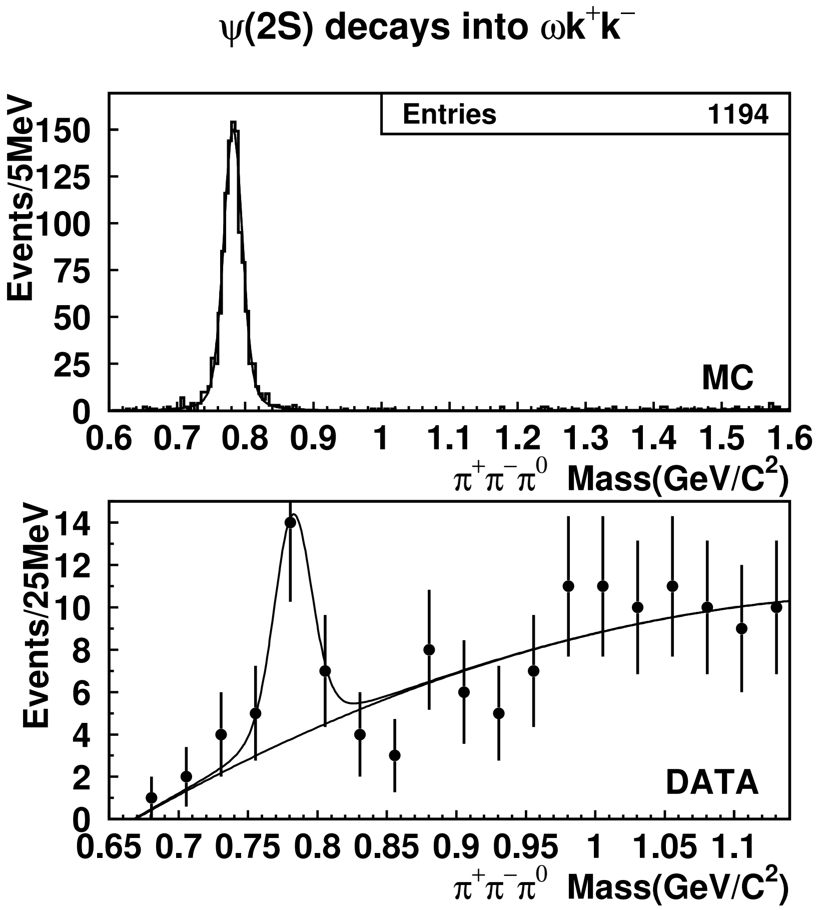


```
================================================================================
I                      Summary Of BWFIT Results                                I
================================================================================
Histogram ID=     1  UnBinned Breit-Wigner Fit using  138 Points
Fit Parameters:Npoly=   3 Nbw=   1 Namp=   0 Range=       .650 To      1.145
Hist. Chisq =      17.42 for   4 params &  15 DF.
Chisquare Probability =  29.42%. Mean and S.D. for pulls:    -.1103     .9268
Likelihood ratio and probability              :      8.254        91.32%
Final Value of Log Likelihood                 :     -116.78
Error Correspond to a Function Chage          :      .50
Phase Space limits for tails corrections      :       .280GEV     2.817GEV
Breit-Wigner efficiency correction factors    :      .986
Include Breit-Wigner tails outside fit region :        .997
Efficiency-corrected events in fit region     :      138.[average eff. :1.000]
---THE FITTED VALUES AND ERRORS OF THE PARAMETERS:---
leg1    Value :  .89841    Error(Cov,-/+):    .143      -.143      .143
leg2    Value : -.21818    Error(Cov,-/+):    .220      -.213      .225
Rate    Value :  .11745    Error(Cov,-/+):    .404E-01 -.384E-01  .422E-01
RESL    Value :  .11980E-01Error(Cov,-/+):    .000E+00 -.638E-02  .607E-02
GAMA    Value :  .84300E-02Error(Cov,-/+):    .000E+00  .000E+00  .000E+00
MASS    Value :  .78234    Error(Cov,-/+):    .614E-02  .000E+00  .000E+00
```

Figure 11: The unbinned B-W fit for $\Psi(2S) \rightarrow \omega K^+K^-$, MC (upper) and DATA (lower)

Fig. 10 show the same physical quatity distributions as Fig. 7. The distributions are similar to those in Fig. 7. The unbinned B-W fit results are shown in Fig. 11, and are listed in Table 3.

2.4.6 $\Psi(2S) \to \phi K^+K^-$, backgrounds from $\Psi(2S) \to \pi^+\pi^-K^+K^-, \pi^+\pi^-\pi^+\pi^-$

With $\phi \to K^+K^-$, 4-C Kinematic fits to the $K^+K^-K^+K^-$ final states are done for the events passing the above general cuts (see Sec. 2.4.1), the probability of fit and that of dE/dX for the selected events are larger than 1%. To remove the backgrounds, the probability of fit plus dE/dX should be greater than those of $\Psi(2S) \to \pi^+\pi^-K^+K^-, \pi^+\pi^-\pi^+\pi^-$. In brief, the cuts are listed as following:

- $\mathrm{CL(4C)}_{K^+K^-K^+K^-} \geq 0.01$, $\mathrm{CL(dE/dX)}_{chrgs} \geq 0.01$,
- $CL(4C + dE/dX)_{K^+K^-K^+K^-} > CL(4C + dE/dX)_{\pi^+\pi^-K^+K^-,\pi^+\pi^-\pi^+\pi^-}$

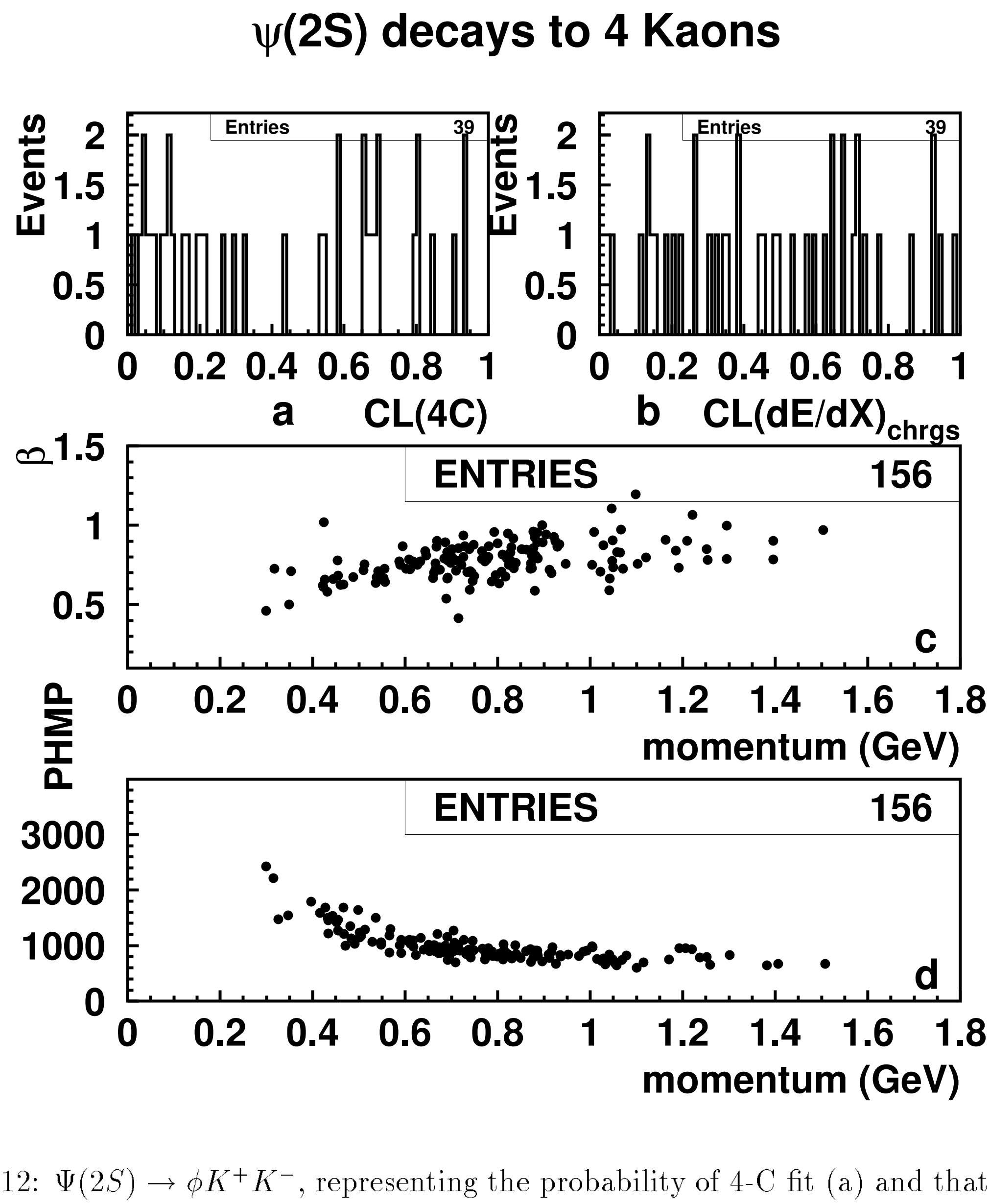

Figure 12: $\Psi(2S) \to \phi K^+K^-$, representing the probability of 4-C fit (a) and that of dE/dX (b), TOF β (c) and dE/dX pulse height (d) v.s momenta.

The Fig. 12 show the distributions of the probability of fit and that of dE/dX, and the TOF and dE/dX information of the selected $K^+K^-K^+K^-$ events. The χ_{s_K} distribution is not shown here for low statistics.

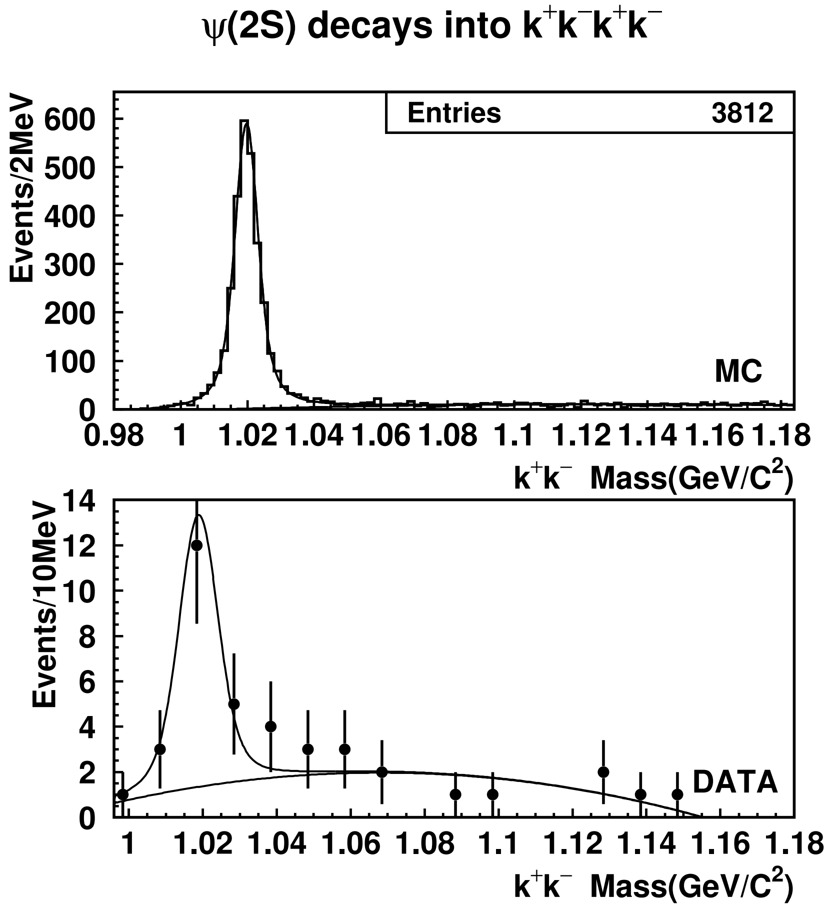


```
==============================================================================
I                      Summary Of BWFIT Results                              I
==============================================================================
Histogram ID=     1  UnBinned Breit-Wigner Fit using   39 Points
Fit Parameters:Npoly=   3 Nbw=   1 Namp=   0 Range=       .996 To      1.180
Hist. Chisq =      12.61 for   5 params &  12 DF.
Chisquare Probability =  39.79%. Mean and S.D. for pulls:     .0893     .8323
Likelihood ratio and probability            :     11.491        48.74%
Final Value of Log Likelihood               :       -87.71
Error Correspond to a Function Chage        :      .50
Phase Space limits for tails corrections    :       .280GEV     2.817GEV
Breit-Wigner efficiency correction factors  :      .964
Include Breit-Wigner tails outside fit region :       .999
Efficiency-corrected events in fit region   :       39.[average eff. :1.000]
---THE FITTED VALUES AND ERRORS OF THE PARAMETERS:---
leg1    Value : -.83550    Error(Cov,-/+):    .354     -.324      .417
leg2    Value : -1.2805    Error(Cov,-/+):    1.01     -1.17      .998
Rate    Value :  .46251    Error(Cov,-/+):    .137     -.137      .142
RESL    Value :  .43203E-02Error(Cov,-/+):    .223E-02 -.197E-02  .333E-02
GAMA    Value :  .44300E-02Error(Cov,-/+):    .000E+00 -.189E-02  .216E-02
MASS    Value :  1.0189    Error(Cov,-/+):    .199E-02  .000E+00  .000E+00
```

Figure 13: the unbinned B-W fit for $\Psi(2S) \to \phi K^+K^-$, the upper for MC, and the lower for DATA

The unbinned B-W fit results are dipicted in Fig. 13, and will be listed in Table 3.

2.4.7 $\Psi(2S) \to \omega p\bar{p}, \eta p\bar{p}$, very low backgrounds from $\Psi(2S) \to \omega K^+K^-, \omega\pi^+\pi^-$

In these two channels, (ω, η) decay into $\pi^+\pi^-\pi^0 \to \gamma\gamma\pi^+\pi^-$. The events of the final states $\gamma\gamma\pi^+\pi^-p\bar{p}$ passing the general cuts (see Sec. 2.4.1) are 5-C fitted with all pairs of photon candidates resonating a π^0 and loop over all possible π/p assignments, the kinematic fit and dE/dX are combined. The events with the lowest value of total χ^2:

$$\chi^2 = \chi^2_{5C-fit} + \sum_i (\chi^2_{s_i dE/dX})$$

are selected, and also required to pass the probability cuts ($\geq 1\%$) for 5-C fit and for the dE/dX (see Sec. 2.4.1). To exclude the backgrounds, the probability of 5-C fit plus dE/dX should be greater than those of $\Psi(2S) \to \omega K^+K^-, \omega\pi^+\pi^-$. The concrete cuts are:

- $CL(5C)_{\omega p\bar{p}} \geq 0.01$, $CL(dE/dX)_{chrgs} \geq 0.01$, $E^{fit}_{\gamma min} > 60MeV$,
- CL(5C+dE/dX)$_{\omega p\bar{p}}$ > CL(5C+dE/dX)$_{\omega K^+K^-, \omega\pi^+\pi^-}$

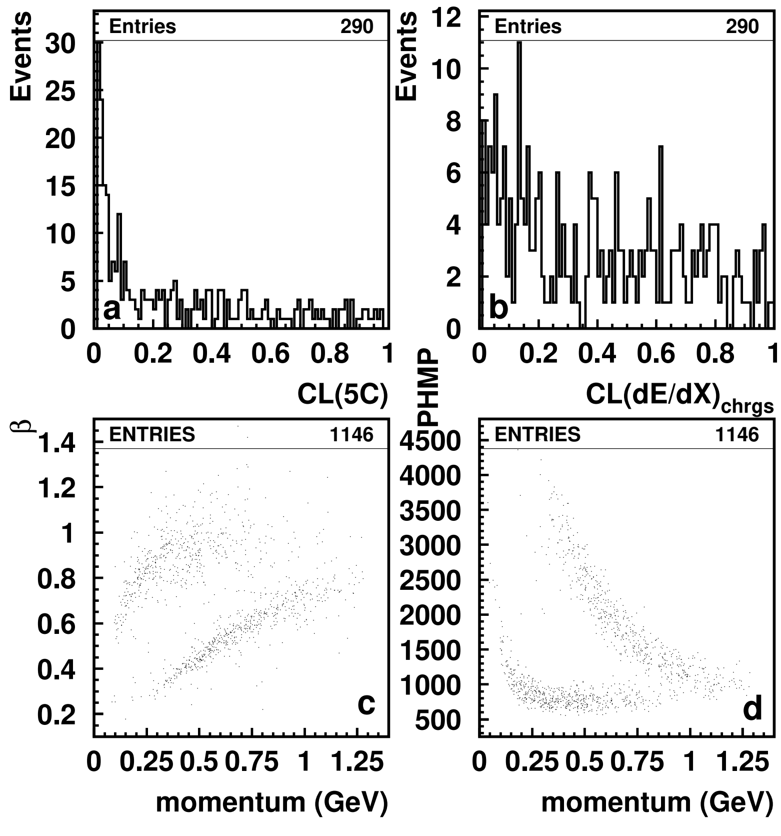

Figure 14: $\Psi(2S) \to \omega p\bar{p}$, probability distributions of 5-C fit (a) and dE/dX (b), TOF β (c) and dE/dX pulse height (d) v.s particle momenta.

Fig. 14 show the some distributions of the selected events, from these figures, we can conclude that there exist good particle seperations for π/p from both TOF and dE/dX at BES.The χ_{s_π} and χ_{s_p} distributions are not presented here because of low statistics, while they are shown in Fig. 16 for $\Psi(2S) \to \gamma\gamma\pi^+\pi^-p\bar{p}$.

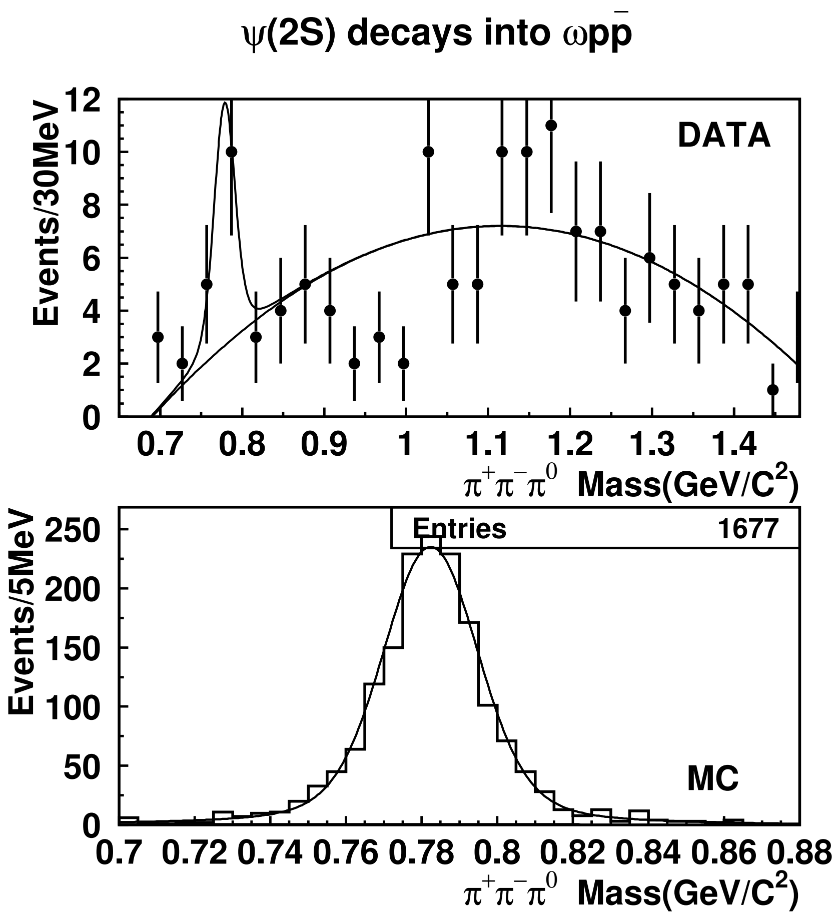


```
==============================================================================
I                      Summary Of BWFIT Results                              I
==============================================================================
Histogram ID=     1  UnBinned Breit-Wigner Fit using  141 Points
Fit Parameters:Npoly=   3 Nbw=   1 Namp=   0 Range=       .600 To      1.500
Hist. Chisq =       61.73 for   4 params &  25 DF.
Chisquare Probability =    .01%. Mean and S.D. for pulls:     .2182    1.4177
Likelihood ratio and probability             :     27.649        32.42%
Final Value of Log Likelihood                :       -40.67
Error Correspond to a Function Chage         :      .50
Phase Space limits for tails corrections     :       .280GEV     2.817GEV
Breit-Wigner efficiency correction factors   :      .991
Include Breit-Wigner tails outside fit region :        .997
Efficiency-corrected events in fit region    :      141.[average eff. :1.000]
---THE FITTED VALUES AND ERRORS OF THE PARAMETERS:---
leg1    Value :  .53926    Error(Cov,-/+):    .954E-01 -.975E-01  .960E-01
leg2    Value : -1.2446    Error(Cov,-/+):    .161      -.146      .174
Rate    Value :  .77920E-01Error(Cov,-/+):    .305E-01 -.283E-01  .327E-01
RESL    Value :  .10900E-01Error(Cov,-/+):    .000E+00 -.647E-02  .653E-02
GAMA    Value :  .84300E-02Error(Cov,-/+):    .000E+00  .000E+00  .000E+00
MASS    Value :  .77859    Error(Cov,-/+):    .638E-02  .000E+00  .000E+00
```

Figure 15: $\Psi(2S) \to \omega p\bar{p}$, the unbinned B-W fit for DATA (upper), MC (lower).

The unbinned B-W fit results are shown in Fig. 15, and are tabulated in Table 3. The signal significance is: $\sqrt{2 \cdot (40.67 - 34.86)} = 3.41\sigma$. Meanwhile 3 events of masses $m_{\pi^+\pi^-\pi^0} = 0.551403, 0.55725, 0.554992 GeV$ forming η are observed with clear signals and the acceptance $\epsilon = 4.13\%$ and $\sigma_\eta = 7.0$ MeV, and the branching ratio is:

$$Br(\Psi(2S) \to \eta p\bar{p}) = (8.36 \pm 4.8 \pm 4.8) \times 10^{-5}$$

where η decays into $\pi^+\pi^-\pi^0$ and the systematic error is conservatively estimated to be same as the statistical error.

2.4.8 $\Psi(2S) \to \pi^0\pi^+\pi^- p\bar{p}, \eta\pi^+\pi^- p\bar{p}$

I analyse these two channels with (π^0, η) decays into $\gamma\gamma$. The final state topology is $\gamma\gamma\pi^+\pi^- p\bar{p}$, the method is same as Sec. 2.4.7, here only 4-C fit is done. The clear π^0, η signals can be seen (Fig. 17). The cuts are:

- $CL(5C)_{\gamma\gamma\pi^+\pi^- p\bar{p}} \geq 0.01$, $CL(dE/dX)_{chrgs} \geq 0.01$, $E^{fit}_{\gamma min} > 50MeV$, [1]

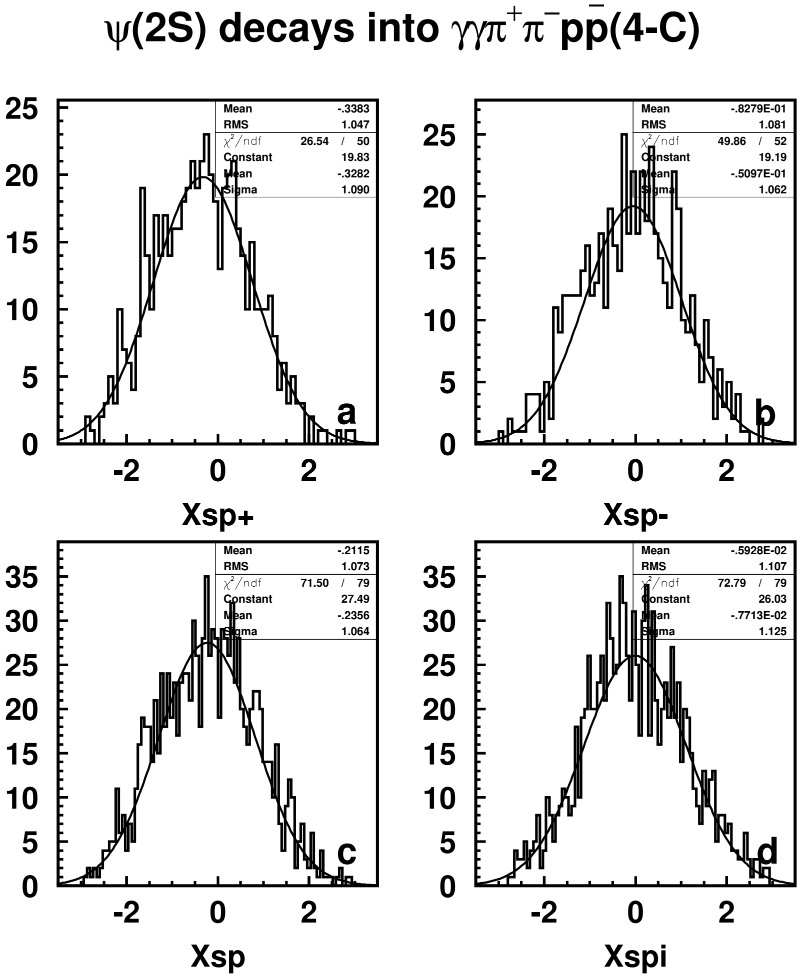

Figure 16: The dE/dX particle separation χ_s distribution for protons, antiprotons and pions in $\Psi(2S) \to \pi^0\pi^+\pi^- p\bar{p}, \eta\pi^+\pi^- p\bar{p}$.

As observed in Sec. 2.4.7, there exists very good π/p seperation in these channels, similar to Fig. 14, I don't show them here, but the distributions of the dE/dX separation χ_s of protons, antiprotons and pions are illustrated in Fig. 16. There is a little left-shift of χ_s for the protons, but the χ_s distributions for pions and antiprotons are quite good (0,1) Gaussian, since there exists difference between the behavior of protons and antiprotons when they pass through the media.

[1] **Note:** Since the energy spectra of photons from these two channels are higher than those from $\Psi(2S)$ decays into $\omega + (\pi^+\pi^-, K^+K^-, p\bar{p})$, so I **lower** the energy cut for photons to 50MeV.

The unbinned B-W fit results are depicted in Fig. 17 and will be listed in Table 3.

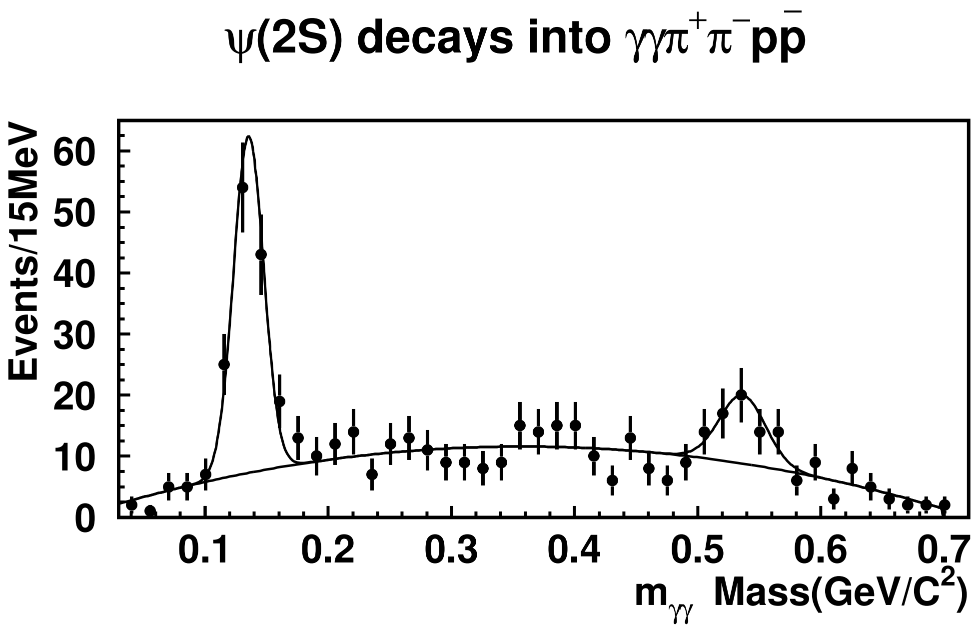


```
==============================================================================
I                     Summary Of BWFIT Results                                 I
==============================================================================
Histogram ID=     1  UnBinned Breit-Wigner Fit using  520 Points
Fit Parameters:Npoly=   3 Nbw=   2 Namp=   0 Range=       .020 To       .700
Hist. Chisq =      27.20 for    6 params &  38 DF.
Chisquare Probability =  90.35%. Mean and S.D. for pulls:    -.0089     .7774
Likelihood ratio and probability           :     26.856        91.18%
Final Value of Log Likelihood              :      -330.73
Error Correspond to a Function Chage       :      .50
Phase Space limits for tails corrections   :       .280GEV     2.817GEV
Breit-Wigner efficiency correction factors :     1.000        1.000
Include Breit-Wigner tails outside fit region :       .000        1.000
Efficiency-corrected events in fit region  :      520.[average eff. :1.000]
---THE FITTED VALUES AND ERRORS OF THE PARAMETERS:---
leg1    Value : -.16733E-01Error(Cov,-/+):    .654E-01 -.671E-01  .649E-01
leg2    Value : -.81885    Error(Cov,-/+):    .751E-01 -.685E-01  .812E-01
Rat1    Value :  .21615    Error(Cov,-/+):    .212E-01 -.208E-01  .215E-01
RES1    Value :  .12200E-01Error(Cov,-/+):    .000E+00 -.150E-02  .151E-02
GAM1    Value :  .00000E+00Error(Cov,-/+):    .000E+00 -.170E-01  .181E-01
MAS1    Value :  .13531    Error(Cov,-/+):    .150E-02 -.619E-02  .623E-02
Rat2    Value :  .67080E-01Error(Cov,-/+):    .176E-01  .000E+00  .000E+00
RES2    Value :  .18700E-01Error(Cov,-/+):    .000E+00  .000E+00  .000E+00
GAM2    Value :  .11800E-05Error(Cov,-/+):    .000E+00  .000E+00  .000E+00
MAS2    Value :  .53638    Error(Cov,-/+):    .615E-02  .000E+00  .000E+00
```

Figure 17: $\Psi(2S) \to \pi^0\pi^+\pi^- p\bar{p}, \eta\pi^+\pi^- p\bar{p}$, the unbinned B-W fit for DATA.

2.4.9 $\Psi(2S) \to \phi p\bar{p}$, very low backgrounds $\Psi(2S) \to K^+K^-K^+K^-, \pi^+\pi^-K^+K^-$

The concrete method is same as $\Psi(2S) \to \phi\pi^+\pi^-$ (cf Sec. 2.4.3). The kinematic fit (4-C) to the $K^+K^-p\bar{p}$ final states is combined with the dE/dX information, the events with the smallest total $\chi^2 = \chi^2_{4C-fit} + \sum_i(\chi^2_{s_i dE/dX})$ are selected, and are required that the probability of 4-C fit and that of the dE/dX are greater than 1%, the probablity of 4-C fit plus dE/dX must be greater than those of $K^+K^-K^+K^-, \pi^+\pi^-K^+K^-$ to exclude the backgrounds. The following are the cuts:

- CL(4C)$_{K^+K^-p\bar{p}} \geq 0.01$, CL(dE/dX)$_{chrgs} \geq 0.01$,
- $CL(4C + dE/dX)_{\phi p\bar{p}} > CL(4C + dE/dX)_{\pi^+\pi^-K^+K^-,\ K^+K^-K^+K^-}$

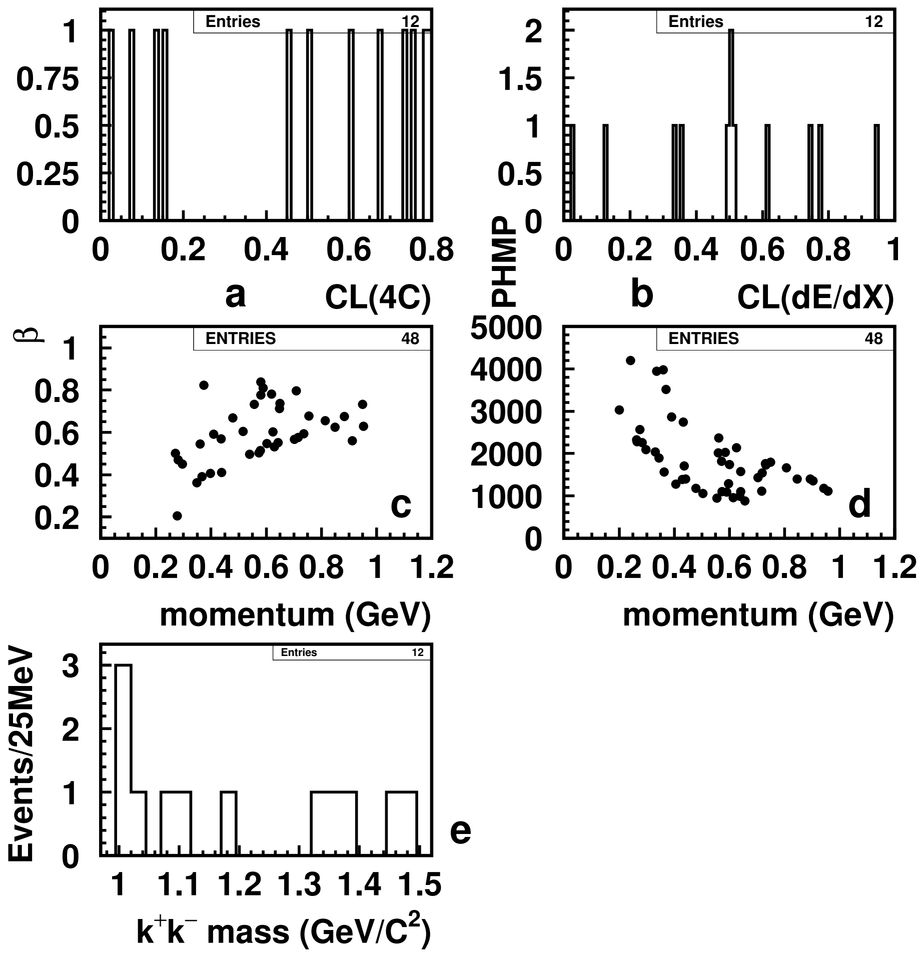

Figure 18: $\Psi(2S) \to \phi p\bar{p}$, probability distributions of 4-C fit (a) and dE/dX (b), TOF β (c) and dE/dX pulse height (d) v.s particle momenta, (e) K^+K^- invariant mass $m_{K^+K^-}$.

Only a few events with $m_{K^+K^-} = 1.01459, 1.00636, 0.999595, 1.04043, 1.092$ GeV at low mass region are observed, Fig. 18 diagram the results. The branching ratio will be given with three events of $m_{K^+K^-} < 1.04$GeV as signals.

2.4.10 Background Study

Use MC samples, let them pass the same event analysis programs to study background.

Table 1: Background Study, the number in the 2nd row is the MC generated event amount.

$\Psi(2S) \to$	Background(s)	Backgrounds $\in (m_R \pm 3\sigma_{m_R})$
$\omega\pi^+\pi^-$	$\omega K^+K^-(30000)$	14
ωK^+K^-	$\omega\pi^+\pi^-(30000)$	23
$\phi\pi^+\pi^-$	$\pi^+\pi^-\pi^+\pi^-(10000)$	0
	$K^+K^-K^+K^-(20000)$	9
ϕK^+K^-	$\pi^+\pi^-K^+K^-(20000)$	7∈(1,1.04)

MC study indicates low backgrounds exist, then B-W fit can not be carried out, we simply regard all events within $m_R \pm 3\sigma_{m_R}$ as backgrounds, so the backgrounds can be neglected after the cuts.

3 Results and Discussion

3.1 Study of the Systematic Errors

After the above analyses, the preliminary results are attained. Meanwhile, Acceptance for each process from MC simulation has been got. The results are listed in Table 3. First, I will presented the study of the systematic errors.

The systematic errors mainly come from the following sources:

(1). the event selection criteria,

(2). the errors of the acceptance and the mass resolution from MC simulation.

(3). the errors of the total number of $\Psi(2S)$,

(4). the errors of ϕ, ω, η and π^0 decay branching ratios used in our calculations.

To gain the systematic errors, let the cuts shift a standard deviation, namely,

- Probality cuts $Prob(dE/dX)_{chrgs}$ and $Prob(fit)$ shift from 0.01 to 0.04.
- photon energy cut $E^{fit}_{\gamma min}$ shifts from $0.06 \Rightarrow 0.05$GeV.
- mass resolution shifts around 10% from the MC determined values.
- polar angle $|cos\theta|$ cut shifts from 0.8 to 0.75.

- the recoil mass m_{recoil} to reject J/ψ background shifts from $m_{J/\psi} \in (3.05, 3.15)$ to $m_{J/\psi} \in (3.00, 3.20)$.

- the dE/dX particle separation within 3σ, i.e, $|\chi_s| < 3$ for each charged track varies from $|\chi_s| < 3$ to $|\chi_s| < 3.5$ for each charged track.

While the others will be directly included in calculating the branching ratios. The branching ratios[12] of the intermediate decay processes used here are listed in Sec. 2.1, they are:
$Br(\phi \rightarrow K^+K^-) = (49.1 \pm 0.8)\%$, $Br(\pi^0 \rightarrow 2\gamma) = (98.798 \pm 0.032)\%$,
$Br(f_0 \rightarrow \pi^+\pi^-) = (78.1 \pm 2.4)\%$, $Br(\eta \rightarrow 2\gamma) = (39.21 \pm 0.34)\%$,
$Br(\omega \rightarrow \pi^+\pi^-\pi^0) = (88.8 \pm 0.7)\%$, $\Gamma_{f_0} = 50MeV$ [33].

But they only leads to small systematic errors.

The contributions to the systematic errors from different error sources are listed as following in Table 2. The errors from the total number of $\Psi(2S)$ $N_{\Psi'}$ ($\sim 8.2\%$) and branching fractions: Br($\phi \rightarrow K^+K^-$)(1.6%), $Br(\pi^0 \rightarrow 2\gamma)(\sim 0.0\%)$, $Br(f_0 \rightarrow \pi^+\pi^-)(3.0\%)$, $Br(\eta \rightarrow 2\gamma)(0.9\%)$ and $Br(\omega \rightarrow \pi^+\pi^-\pi^0)(0.8\%)$ are directly included in the calculations of the total systematic errors, and not listed in Table 2, the quadratic sumation from each source is also listed in this table. For calculations of some ratios (see Sec. 3.3), the systematic errors from the error of $N_{\Psi'}$ cancels, the the quadratic sumation except the error of $N_{\Psi'}$ is also listed in the same table. In addition, the m_ϕ shift leads to 3.5% error for the branching ratio of $\Psi(2S) \rightarrow \phi f_0$.

Table 2: The contributions from the different error sources in percentage (%).

Error sources	$\omega\pi^+\pi^-$	ωK^+K^-	$\phi\pi^+\pi^-$	ϕK^+K^-	ϕf_0	$\omega p\bar{p}$	$\phi p\bar{p}$	$\pi^0\pi^+\pi^-p\bar{p}$	$\eta\pi^+\pi^-p\bar{p}$
CL(fit)$\rightarrow$0.04	1.6	7.8	3.3	18.3	2.8	3.3	7.3	0.5	13.6
CL(dE/dX)$\rightarrow$0.04	6.6	14.7	0.6	5.8	2.5	4.7	2.7	2.8	1.1
$E^{fit}_{\gamma min} 50 \Longrightarrow 60MeV$	5.1	12.4				8.1		4.0	0.6
$m_{J/\psi} \in (3.00, 3.20)$	1.6	12.6	0.1	5.4	$\sim 0.$	14.6	$\sim 0.$	9.4	9.1
$\lvert cos\theta\rvert < 0.75$	0.1	17.0	10.5	9.6	5.2	12.9	20.3	2.0	19.3
$N_{\{\lvert\chi_s\rvert<3.5\}} = 4$	1.5	2.3	0.8	7.2	0.8	2.3	1.0	3.3	9.1
$\sigma_m \sim 10\%$	1.0	3.0	0.3	$\sim$0.0	0.0	1.8	$\sim 0.$	3.0	4.5
acceptance	1.9	0.8	0.4	1.0	0.1	0.9	0.2	0.9	0.9
all sum	12.2	31.0	13.9	24.7	11.6	23.6	23.3	14.3	28.5
sum except $Er_{N_{\{\Psi'\}}}$	9.0	29.9	11.2	23.4	8.2	22.1	21.8	11.7	27.3

The main contributions to the systematic errors for each decay channel from different sources are respectively discussed as following:

- $\Psi(2S) \to \omega\pi^+\pi^-$: the systematic error overwhelmingly comes from the error in the total number of $\Psi(2S)$.

- $\Psi(2S) \to \omega K^+K^-$: several cuts considerably contribute to the systematic error. Some cuts, such as CL(5C)→0.04, CL(dE/dX)→0.04, $E^{fit}_{\gamma min} = 60 \to 50MeV$, $m_{J/\psi} \in (3.00, 3.20)$, they hardly affect the signals, but mainly affect the shape of background which lead to large contributions to the systematic errors. The cut $|cos\theta| < 0.75$ which affects both the acceptance and the shape of background causes greater contribution to the systematic error. With greater statistic, the cuts will have much less influence on the shape of background, of course the systematic errors will greatly decrease too. So the greater the statistic, the much lower both statistical errors and systematic errors (and onwards).

- $\Psi(2S) \to \phi\pi^+\pi^-$: The systematic error is mainly from the error in the total number of $\Psi(2S)$ and the error from the cut $|cos\theta| < 0.75$ which bring about a bit lower acceptance.

- $\Psi(2S) \to \phi K^+K^-$: The three largest contributions to systematic error are the error in the total number of $\Psi(2S)$ and the error caused by the cut CL(4C)→0.04 which affects the low mass region of $m_{K^+K^-}$ and the shape of background so that it contributes large error, and the error from $|cos\theta|$ cut which brings a little lower acceptance.

- $\Psi(2S) \to \phi f_0$: The systematic error predominantly comes from the error in the total number of $\Psi(2S)$.

- $\Psi(2S) \to \omega p\bar{p}$: the cuts: $|cos\theta| < 0.75$ and $m_{J/\psi} \in (3.0, 3.2)$ both affect the signals and the shape of background, because of low statistic, they will sensitively contribute large errors to the systematic error together with the error in the total number of $\Psi(2S)$.

- $\Psi(2S) \to \phi p\bar{p}$: only $|cos\theta| < 0.75$ reduces one signal, all other cuts have no influence on the signals.

- $\pi^0\pi^+\pi^-p\bar{p}$: The systematic error dominantly comes from the error in the total number of $\Psi(2S)$ and the error from the cut: $m_{J/\psi} \in (3.0, 3.2)$ which reduces quite a few signals.

- $\eta\pi^+\pi^-p\bar{p}$: The main contributions to the systematic error are from the errors caused by the cuts: $CL(4C) > 0.04$ and $|cos\theta| < 0.75$ which mainly affect the shape of background so that large errors were produced.

From the above table, the total systematic errors are compatible to the statistical errors.

3.2 Preliminary Results

Table 3: Measurements of the $\Psi(2S)$ decay Branching Ratios. (Note: Γ_{f_0}=50MeV), Units: σ_m ~MeV, m_R ~GeV, and ϵ_{acc}, Er_{st} and Er_{sys} in percentage(%).

Ψ(2S) $\Rightarrow$	N_{gen}	ϵ_{acc}	N_{obs}	Er_{st}	Er_{sys}	σ_m	m_R(GeV)	Br($\times 10^{-5}$)
$\omega\pi^+\pi^-$	30000	5.34	79.3±10.2	12.9	12.2	10.3	0.7831±0.002	$44.7 \pm 5.7 \pm 5.4$
ωK^+K^-	30000	3.86	16.2±5.5	34.0	31.0	12.0	0.7823±0.006	$12.6 \pm 4.3 \pm 3.9$
$\phi\pi^+\pi^-$	20000	17.61	57.4±7.2	12.5	13.9	2.1	1.0185± 0.001	$17.6 \pm 2.2 \pm 2.4$
ϕK^+K^-	20000	15.94	18.1± 5.3	29.3	24.7	4.3	1.0189±0.002	$6.10 \pm 1.79 \pm 1.51$
ϕf_0	10000	21.27	20.3±5.2	25.6	11.6	9.4	0.9834±0.008	$6.57 \pm 1.68 \pm 0.76$
$\omega p\bar{p}$	30000	5.52	11.0±4.3	39.1	23.6	10.9	0.7786±0.006	$6.00 \pm 2.34 \pm 1.41$
$\phi p\bar{p}$	20000	18.69	3.0±1.7	57.7	23.3	2.2		$0.86 \pm 0.50 \pm 0.20$
$\pi^+\pi^-\pi^0 p\bar{p}$	20000	7.80	112.4±11.0	9.8	14.3	12.2	0.1353±0.002	38.5±3.7 $\pm$ 5.5
$\eta\pi^+\pi^- p\bar{p}$	20000	9.14	35.0±9.2	26.3	28.5	18.7	0.5364±0.006	25.8±6.8 $\pm$ 7.3
$\eta p\bar{p}$	20000	4.13	3 ± 1.7	57.7	57.7	7.0	0.5545±0.004	8.36±4.8 $\pm$ 4.8

The preliminary results are listed in Table 3. From the table, we can see that the fitted masses of resonances for the processes $\Psi(2S) \to \omega\pi^+\pi^-$, ωK^+K^-, $\phi\pi^+\pi^-$, ϕK^+K^-, $\pi^0\pi^+\pi^- p\bar{p}$ and ϕf_0 accords very well with the PDG values[12], and those for $\omega p\bar{p}$ and $\eta\pi^+\pi^- p\bar{p}$ are also consistent with the PDG values but within a bit larger errors.

3.3 Tests of the OZI rule

Using these results, we can test the OZI rule and QCD "15%" rule (cf Sec. 1.2). The ratios of the branching fraction of $\Psi(2S) \to \phi X$ to that of $\Psi(2S) \to \omega X$ are predicted [25]:

$$R_{(\phi X/\omega X)} = \frac{Br(\Psi(2S) \to \phi X)}{Br(\Psi(2S) \to \omega X)} > \frac{Br(J/\psi \to \phi X)}{Br(J/\psi \to \omega X)} = 0.14$$

and the Large N_C QCD predicts the relative width of DOZI processes to that of the SOZI processes is about $1/N_C^2 \sim 1/9$:

For the above channels involving ω, ϕ production:

$$R_{(\phi\pi^+\pi^-/\omega\pi^+\pi^-)} = \frac{Br(\Psi(2S) \to \phi\pi^+\pi^-)}{Br(\Psi(2S) \to \omega\pi^+\pi^-)} = (39.3 \pm 7.0 \pm 6.0)\%$$

$$R_{(\phi K^+K^-/\omega K^+K^-)} = \frac{Br(\Psi(2S) \to \phi K^+K^-)}{Br(\Psi(2S) \to \omega K^+K^-)} = (48.4 \pm 21.7 \pm 18.4)\%$$

$$R_{(\phi p\bar{p}/\omega p\bar{p})} = \frac{Br(\Psi(2S) \to \phi p\bar{p})}{Br(\Psi(2S) \to \omega p\bar{p})} = (14.5 \pm 9.0 \pm 4.4)\%$$

The results are comparable with the predictions of the perturbative QCD and the large N_C QCD[2].

While for the J/ψ hadronic decays:

$$\frac{Br(J/\psi \to \phi\pi^+\pi^-)}{Br(J/\psi \to \omega\pi^+\pi^-)} = (11.4 \pm 2.4)\%$$

$$\frac{Br(J/\psi \to \phi K^+K^-)}{Br(J/\psi \to \omega K^+K^-)} = (112.2 \pm 40.6)\%$$

$$\frac{Br(J/\psi \to \phi p\bar{p})}{Br(J/\psi \to \omega p\bar{p})} = (3.5 \pm 1.3)\%$$

the ratios of J/ψ and $\Psi(2S)$ hadronic decays are confict with the perturbative QCD predictions within errors.

The OZI violation factors for $\Psi(2S)$ decays, the above ratios to the naive phenomenological $\omega \sim \phi$ mixing model prediction $(1.0 \sim 4.2) \times 10^{-3}$, are:

$$V_{(\phi\pi^+\pi^-/\omega\pi^+\pi^-)} = \frac{0.393}{4.2 \times 10^{-3}} = 93.6 \pm 16.7 \pm 14.3$$

$$V_{(\phi K^+K^-/\omega K^+K^-)} = \frac{0.484}{4.2 \times 10^{-3}} = 115.3 \pm 51.7 \pm 43.8$$

$$V_{(\phi p\bar{p}/\omega p\bar{p})} = \frac{0.145}{4.2 \times 10^{-3}} = 33.9 \pm 21.5 \pm 10.5$$

where the systematic error from the total number of $\Psi(2S)$ cancels in these ratios.

The strong OZI violation with a factor of about two order of magnitude higher w.r.t. the naive phenomenological $\omega \sim \phi$ mixing model is observed in $\Psi(2S) \to \phi\pi^+\pi^-$, $\omega\pi^+\pi^-$, ϕK^+K^-, ωK^+K^-, but for $\Psi(2S) \to \omega p\bar{p}$, $\phi p\bar{p}$, the violation is not seriously broken as $\Psi(2S)$ decays into $\phi\pi^+\pi^-$ and $\omega\pi^+\pi^-$, ϕK^+K^- and ωK^+K^-. Moreover the strong DOZI violation in $\Psi(2S) \to \phi\pi^+\pi^-$, $\omega\pi^+\pi^-$ is also observed with a much larger factor of about two order of magnitude, while for such DOZI process in J/ψ decays, the factor is

$$\frac{Br(J/\psi \to \phi\pi^+\pi^-)}{Br(J/\psi \to \omega\pi^+\pi^-) \times 4.2 \times 10^{-3}} = \frac{8.0 \times 10^{-4}}{7.2 \times 10^{-3} \times 4.2 \times 10^{-3}} = 26.5 \pm 5.4$$

The branching ratios are taken from [12]. Therefore the DOZI violation is much stronger in $\Psi(2S)$ decays than in J/ψ decays.

[2]The combined errors of the ratios are calculated in the form:

$$\sigma = \sqrt{(\frac{\partial f}{\partial x_1})^2\sigma_{x_1}^2 + (\frac{\partial f}{\partial x_2})^2\sigma_{x_2}^2 + \cdots + (\frac{\partial f}{\partial x_m})^2\sigma_{x_m}^2}.$$

Where f is the function of the independent random variables $x_1, x_2, \cdots x_m$ and σ_{x_m} is the standard deviation of the random variable x_m. Simply for the function $f = constant \times x/y$ of two independent variables x, y,

$$\frac{\sigma}{\langle f \rangle} = \sqrt{\frac{\sigma_x^2}{x^2} + \frac{\sigma_y^2}{y^2}}.$$

Where $\langle f \rangle$ is the expectation of function f.

The comparisons show that the naive phenomenological $\omega \sim \phi$ mixing model poorly describe the processes of $\Psi(2S)$ hadronic decays involving ω and ϕ. It means that these decay modes do not proceed via $\omega \sim \phi$ mixing mechanism. The perturbative QCD and large N_C QCD give good qualitative description of these processess.

3.4 Tests of QCD "15%" Rule

Perturbative QCD predicts[11] that

$$Q_h = \frac{Br(\Psi' \to h)}{Br(J/\psi \to h)} = \frac{Br(\Psi' \to e^+e^-)}{Br(J/\psi \to e^+e^-)} = (14.7 \pm 2.3)\%$$

According to the new measurements of the above branching ratios and the method from the PDG tables[12] to quadratically combine the statistical and systematic errors, we can test QCD "15%" rule, the Q_h's are:

$$Q_{\omega\pi^+\pi^-} = \frac{4.47 \times 10^{-4}}{7.2 \times 10^{-3}} = (6.3 \pm 1.4)\%$$

$$Q_{\omega K^+K^-} = \frac{1.26 \times 10^{-4}}{7.4 \times 10^{-4}} = (17.0 \pm 9.6)\%$$

$$Q_{\phi K^+K^-} = \frac{6.10 \times 10^{-5}}{8.3 \times 10^{-4}} = (7.3 \pm 3.0)\%$$

$$Q_{\phi\pi^+\pi^-} = \frac{1.76 \times 10^{-4}}{8.0 \times 10^{-4}} = (22.0 \pm 5.3)\%$$

$$Q_{\phi f_0} = \frac{6.57 \times 10^{-5}}{3.2 \times 10^{-4}} = (20.5 \pm 8.1)\%$$

$$Q_{\omega p\bar{p}} = \frac{6.00 \times 10^{-5}}{1.3 \times 10^{-3}} = (4.6 \pm 2.2)\%$$

$$Q_{\phi p\bar{p}} = \frac{0.86 \times 10^{-5}}{4.5 \times 10^{-5}} = (18.9 \pm 13.4)\%$$

$$Q_{\pi^+\pi^-\pi^0 p\bar{p}} = \frac{3.85 \times 10^{-4}}{2.3 \times 10^{-3}} = (16.7 \pm 7.1)\%$$

$$Q_{\eta p\bar{p}} = \frac{8.36 \times 10^{-5}}{2.09 \times 10^{-3}} = (4.00 \pm 4.00)\%$$

$$Q_{\eta\pi^+\pi^- p\bar{p}} = \frac{2.58 \times 10^{-4}}{\mathrm{NoPDGdata}} =?$$

Where the corresponding J/ψ decay branching ratios are taken from PDG[9, 12]. From the above Q_h's, we can see that for $\Psi(2S) \to \omega\pi^+\pi^-$, ϕK^+K^-, $\omega p\bar{p}$ and $\eta p\bar{p}$, the ratios of $\Psi(2S)$ hadronic decay branching fractions to those of J/ψ is smaller by a factor of 2 with respect to perturbative QCD predictions, while for ωK^+K^-, $\phi\pi^+\pi^-$, ϕf_0, $\phi p\bar{p}$ and $\pi^0\pi^+\pi^- p\bar{p}$, the ratios are consistent with theoritical predictions within errors.

4 Summary

For the first time, the branching ratios of $\Psi(2S)$ decays into $\omega\pi^+\pi^-$, $\phi\pi^+\pi^-$, ωK^+K^-, ϕK^+K^-, ϕf_0, $\omega p\bar{p}$, $\pi^0\pi^+\pi^-p\bar{p}$, $\eta\pi^+\pi^-p\bar{p}$, $\phi p\bar{p}$ and $\eta p\bar{p}$ are given. Through these measurements, the strong OZI and DOZI violation by a factor of two order of magnitude in $\Psi(2S) \to \phi\pi^+\pi^-$, $\omega\pi^+\pi^-$, ϕK^+K^- and ωK^+K^- is observed in contrast to the phenomenologically universal $\omega \sim \phi$ mixing model, while this violation is not serious in $\Psi(2S) \to \omega p\bar{p}$ and $\phi p\bar{p}$. It shows that this model does not give good interpretation of the $\Psi(2S)$ hadronic decays into ω and ϕ. It means that $\Psi(2S)$ hadronic decays into ω and ϕ do not proceed via $\omega \sim \phi$ mixing. The results qualitatively accord well with the perturbative QCD and large N_C QCD predictions, and we are hoping for precisely dynamical quantitative calculation.

The QCD "15%" rule is also tested with these newly measured $\Psi(2S)$ decay branching ratios. Among these channels, the ratios Q_h's are smaller by a factor of 2 in $\Psi(2S) \to \omega\pi^+\pi^-$, ϕK^+K^-, $\omega p\bar{p}$ and $\eta p\bar{p}$, while are consistent with QCD predictions in $\Psi(2S) \to \omega K^+K^-$, ϕf_0, $\pi^0\pi^+\pi^-p\bar{p}$, $\phi p\bar{p}$ and $\phi\pi^+\pi^-$ within errors.

References

[1] J.F. Donoghue, E. Golowich, B. R. Holstein, Dynamics of Standard Model.

[2] N. Cabbibo, Physical Review Letters **10**, 531 (1963).

[3] B. J. Bjorken and S. L. Glashow, Physics Letters **B11**, 255 (1964).

[4] S. L.G Glashow, J. Iliopoulos, L. Maiani, Physical Review **D2**, 1285 (1970).

[5] J. J. Aubert et al., Physical Review Letters **33**, 1404 (1974); J. E. Augustin et al., Physical Review Letters **33**, 1406 (1974);

[6] C. Bacci et al., Physical Review Letters **33**, 1408 (1974).

[7] G. S. Abrams et al., Physical Review Letters **33**, 1453 (1974); P. A. Rapidis et al., Physical Review Letters **39**, 526 (1977).

[8] S. Okubo, Physics Letters **B5**, 165 (1963); G. Zweig, CERN-preprints CERN-TH-401,402,412(1964); J. Iizuka, Prog. Theor. Phys. Suppl., **21** (1966) 37.

[9] A. Seiden, H. F.-W. Sadrozinski, and H. E. Haber, Physical Review **D38**, 824 (1988).

[10] M. E. B. Franklin et al., Physical Review Letters **51**, 963 (1983).

[11] T. Applequist and D. Politzer Physical Review Letters **34**, 43 (1975).

[12] Particle Data Group, R. M. Barnet et al., Physical Review **D54**, 1 (1996).

[13] J. Z. Bai et al., BES Coll., $\Psi(2S)$ Hadronic Decays to Vector Tensor Final States, accepted for publication in Physical Review Letters;Y. S. Zhu, in Proceedings of the 28th International Conference on High Energy Physics. ed. Z. Adjuk and A. K. Wroblewski, World Scientific, 1997.

[14] W. S. Hou and A. Soni, Physical Review Letters **50**, 569 (1983);
G. Karl and W. Roberts, Physics Letters **B144**, 243 (1984);
S. J. Brodsky et al., Physical Review Letters **59**, 631 (1987);
M. Chaichian et al., Nuclear Physics **B323**, 75 (1989);
S. S. Pinsky, Physics Letters **B236**, 479 (1990);
X. Q. Li et al., Physical Review **D55**, 1241 (1997);
S. J. Brodsky and M. Karliner, Physical Review Letters **78**, 468 (1997);
Yu-Qi Chen and Eric Braaten, Physical Review Letters **80**, 5060 (1998).

[15] C. Amsler et al., Physics Letters **B346**, 363 (1995); A. Bertin et al., Physics Letters **B388**, 450 (1996); A. Ferrer et al., Physics Letters **B394**, 395 (1997).

[16] V. E. Markushin and M. P. Locher, Eur. Phys. J. **A1**,91 (1998); V. E. Markushin, Nucl. Phys. Proc. Suppl. **56A**, 303 (1997); B. S. Zou, Phys. Atom. Nucl. **59** 1427 (1996) and references therein.

[17] J. Ellis et al., Physics Letters **B353**, 319 (1995); J. Ellis, hep-ph/9611208.

[18] J. Ellis and M. Karliner, Physics Letters **B313**, 131 (1993).

[19] N. N. Achasov et al., Inter. J. Modern Physics **A Vol. 7, No. 14** (1992) 3187.

[20] H. J. Lipkin, Physics Letters **B60**, 371 (1976).

[21] D. Coffman et al, Mark III Coll., Physical Review **D38**, 2695 (1988), Erratum-ibid.D40:3788,1989.

[22] H. J. Lipkin, Nuclear Physics **B244**, 147 (1984) and references therein.

[23] R. Delbourgo, Dongsheng Liu and M. D. Scadron, hep-ph/9811474; V. M. Aulchenko et al., hep-ex/9807016.

[24] I. J. Muzinch and F. E. Paige, Physical Review **D21**, 1151 (1980).

[25] C. Gilain and F. Hayot, Nuovo Cimento **A41** (1977) 271.

[26] W. F. Palmer and S. S. Pinsky, Physical Review **D14**, 1916 (1976).

[27] R. E. Marshak, Conceptual Foundations of Modern Particle Physics, **Sec. 5.4b**, "Large N_C limit in QCD and the OZI rule", World Scientific, 1993.

[28] MINUIT Reference Manual, CERN Program Library Long Writeup **D506**.

[29] J. Z. Bai et al., BES Coll., Nuclear Instruments and Methods **A344**, 319 (1994).

[30] N.N. Achasov, hep-ph/9803292 and references therein; M. C. Birse et al., editors, HADRON'95, pp454-456, the 6th International Conference on Hadron Spectroscopy, Manchester, UK, Jul 10 - 14, 1995; M. Harada et al., Physical Review **D54**, 1991 (1996), and references therein; N. A. Törnqvist, Zeit. Physik **C68**, 291 (1993); C. A. Dominguez and N. Paver, Zeit. Physik **C39**, 39 (1988); G. Janssen et al., Physical Review **D52**, 2690 (1995).

[31] F. E. Close et al., Physics Letters **B319**, 291 (1993).

[32] A. Falvard et al., Physical Review **D38**, 2706 (1988).

[33] M. P. Locher, V. E. Markushin and H. Q. Zheng, Eur. Phys. J. **C4**, 317(1998), the paper cited $\Gamma_{f_0} = 47 \pm 9 MeV$ from Review of Particle Physics, Physical Review **D54**, 1 (1996)[12]; P. Lebrun et al, FERMILAB-CONF-97-388-E; A. A. Kondashov, hep-ph/9811207.